The Thesis Committee for Jason Allan Abedania Hernandez
Certifies that this is the approved version of the following thesis:

Development and Laboratory Testing of Ultra High Performance Concrete

APPROVED BY
SUPERVISING COMMITTEE:

Supervisor:

Kevin J. Folliard

Thanos Drimalas

Development and Laboratory Testing of Ultra High Performance Concrete

by

Jason Allan Abedania Hernandez, B.S

Thesis

Presented to the Faculty of the Graduate School of

The University of Texas at Austin

in Partial Fulfillment

of the Requirements

for the Degree of

Master of Science in Engineering

The University of Texas at Austin

December 2016

Dedication

This thesis is dedicated to my family, friends, and loving wife

Acknowledgements

This thesis would not have been possible without the support of my friends, family and colleagues.

I would like to first thank my parents Janet and Angelito Hernandez. I would not be where I am right now without your love and support. My dad, who almost ten years to the date of writing this paper passed away still continues to be my source of motivation. To my mom, thank you for your love regardless of the situation or circumstance. Also, to my older brother AJ, thank you for believing in me and allowing me to pursue my dreams.

I would also like to thank my supervising professor, Dr. Kevin Folliard. Thank you for your wisdom and guidance throughout this process of completing my graduate degree. Your engaging teaching style and passion for concrete made this a rewarding experience and sparked a thirst of knowledge that will continue throughout my career.

I would also like to extend my gratitude to Dr. Thanos Drimalas. You went beyond what was expected and supported me throughout every phase of this research project. Thank you for your patience and willingness to help to ensure the success of this project.

Thank you to all the staff and students from the Lab. Mike, Racheal, Bruno, Jose, Nick, Jeremy, Sanjida, Gwen, Ryan, and Saif, I can't thank you all enough for the help in mixing, testing and overall support of my project. I would also like to thank the undergraduate help I received. Chris, Raul, and Zia, neither of you were assigned to my project initially but found time to assist me and I am grateful for every second you were able to help.

Finally, I would like to thank my wife Ana. You have been patient, caring, loving, faithful, and supportive during this process. I can't thank you enough for supporting me

not only at home but at the lab when I needed an extra hand. This thesis would not have been possible without you. Having you by my side made this whole experience worth it.

Abstract

Development and Laboratory Testing of Ultra High Performance Concrete

Jason Allan Abedania Hernandez, M.S.E

The University of Texas at Austin, 2016

Supervisor: Kevin J. Folliard

Ultra-High Performance Concrete (UHPC) is an emerging material technology that exhibits a combination of high compressive strength, high tensile strength, high toughness and ductility, and improved durability when compared to normal concrete. These characteristics lead to applications in bridge structures across the various department of transportations in the country.

The objective of this research was to characterize proprietary and non-proprietary UHPC mixtures in the laboratory, with the ultimate goal aimed at implementing UHPC in bridge applications in Texas, particularly for field-cast connections and closure pours.

Table of Contents

List of Tables

List of Figures

Chapter 1: Introduction

1.1 Background

Over the past decade, Ultra High Performance Concrete (UHPC) has emerged as a promising material in the use of highway bridge structures for its enhanced mechanical and durability properties. In general, this material can exhibit compressive strengths of 193 MPa (28 ksi), tensile strengths of 9.0 MPa (1.3 ksi), and elastic modulus of 52.4 GPa (7,600 ksi) (Graybeal, 2006). In 2006, a report published by the Federal Highway Association (FHWA) entitled *Material Property Characterization of Ultra-High Performance Concrete* increased awareness of UHPC and led to a variety of field trials performed by state departments of transportation (DOTs).

The research described in this thesis is the initial phase of a project at the University of Texas at Austin that is funded by the Texas Department of Transportation (TxDOT). This preliminary laboratory work will be followed up with more comprehensive laboratory evaluations, including flexural toughness and long-term durability (e.g., alkali-silica reaction, external sulfate attack, corrosion, etc.). The overall goal of the project is to characterize proprietary and non-proprietary UHPC mixtures through fresh and hardened concrete testing, with primary focus in this thesis on strength (tensile and compressive) and elastic modulus. Materials used in the non-proprietary mixes included condensed silica fume, calcined clay (metakaolin), steel fibers, and polyvinyl alcohol (PVA fibers).

1.2 Organization of thesis

This thesis is organized and presented as shown below:

Chapter 1 is a brief introduction and description of the overall project objectives.

Chapter 2 is a review of UHPC research done in the past. This includes a review of laboratory and field applications of UHPC.

Chapter 3 describes the experimental approach for the project. All of the tests were conducted following applicable American Society for Testing and Materials (ASTM) standard test procedures. However, due to the unique nature of UHPC, some tests were modified as recommended by past research in order to capture the behavior of the material. This chapter includes discussion of the modifications. The tests performed include the following:

- ASTM C 109 *Compressive Strength of Hydraulic Cement Mortars*
- ASTM C 469 *Static Modulus of Elasticity and Poisson's Ratio of Concrete in Compression*
- ASTM C 496 *Splitting Tensile Strength of Cylindrical Concrete Specimens*
- ASTM C 1497 *Flow of Hydraulic Cement Mortar*

This chapter also includes an analysis of the results from the experimental section including a comparison of data from other studies in order to obtain better perspective on the material.

Chapter 4 presents the conclusion of the report and also discusses potential future projects in the area of UHPC.

Chapter 2: Review of Ultra High Performance Concrete

2.1 Introduction

UHPC is a composite material with similar cement hydration reactions as conventional concrete. A typical UHPC mix includes cement, fine aggregates, supplementary cementitious materials (SCM), steel fibers, and a high range water reducer (HRWR). The materials are all specifically chosen to achieve increased mechanical and durability properties. Currently, there are a number of proprietary UHPC mixes available or being developed in the market (Graybeal, 2014).

2.2 Microstructure of Concrete

Although unique as a material, UHPC has similar hydration products and properties as conventional concrete. This next section acts as overview of the microstructure of concrete to help better understand the reasoning behind the mix design and materials of UHPC.

2.2.1 Hydrated Cement Paste Products

The main product of the hydrated cement paste in a concrete mix is calcium silicate hydrate, commonly abbreviated as C-S-H. This product makes up 50 to 60 % of the volume of solids in a hydrated cement paste (Mehta and Monteiro, 2014). More importantly, C-S-H is the main hydration responsible for the binding capacity, strength, and durability properties of the paste and concrete as a whole. The structure of C-S-H is not well-defined but can be resolved with the use of scanning electron microscopy (SEM). Due to the structure, not being well defined, the CaO/SiO_2 ratio varies between 1.2 to 2.3 in addition to the amount of water (Mehta and Monteiro, 2014). However, what is known about C-S-H is that it has a very high surface area and are held together by strong van der waals'

forces (Mehta and Monteiro, 2014). These van der waals' forces are primarily the source of the strength of the material.

The next main hydration product is calcium hydroxide ($Ca(OH)_2$) commonly denoted as CH. These products take up 20 to 25 % of the volume of solids in the hydrated cement paste (Mehta and Monteiro, 2014). Unlike C-S-H, CH is a well-defined cement hydration product. Also unlike C-S-H, CH is a large plate like structure with low surface area and a low contribution to the strength and durability of the hydrated cement (Mehta and Monteiro, 2014). The lower surface area gives CH less adhesion capacity compared to the higher surface area found in C-S-H. In the most general terms, CH is more detrimental than beneficial when looking at optimizing the strength of the concrete material.

In addition to these two hydration products, there are also calcium sulfo-aluminate hydrate products which take up 15 to 20 % of the solid volume in hydrated cement paste (Mehta and Monteiro, 2014). In comparison, these products are lower in amount and are less critical in the mechanical properties of the material. However, they are critical when considering durability issues such as sulfate attack.

2.2.2 Development of Microstructure

During hydration, the C-S-H forms around the cement grains whereas the CH and other products form in the space between the cement grains. Over time, the C-S-H formed around the cement grain grows to the point of touching one another which is commonly known to be the point of initial set. Any space not occupied by a hydration product or cement grain in the hydrated paste is considered to be a void or capillary porosity. Since it has been established that the strength of concrete comes from the hydrated cement paste, it can be concluded that any area without paste in the material negatively effects the strength. In order to reduce porosity, there are some factors to consider.

First, the amount of curing is important in decreasing porosity and increasing the degree of hydration shown in Figure 1 (Young et al. 1998). The more the concrete is cured, the more hydration products are allowed to form, hence reducing porosity. In addition, increasing the degree of hydration or the amount of cement hydrated is also achieved by more curing. Second, decreasing the water to cement ratio (W/CM) also decreases the porosity as shown in Figure 2 (Mehta and Monteiro, 2014). Figure 2 also shows how much easier it is to achieve a lower capillary porosity with a lower water to cement ratio and a higher degree of hydration.

Figure 1: Effect of curing on capillary porosity and degree of hydration (Young et al. 1998)

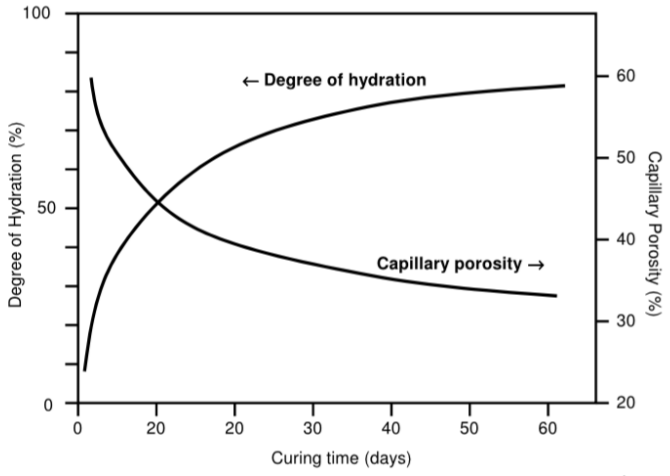

Figure 2: Effect of W/CM on capillary porosity (Mehta and Monteiro 2014)

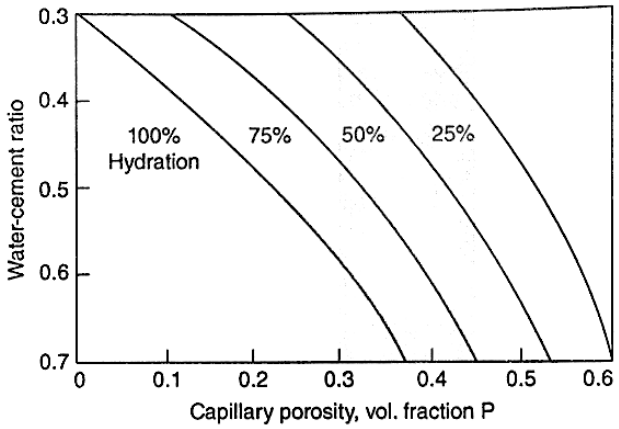

The relationship of compressive strength and porosity was first researched by Powers and Brownyard. They concluded that portland cement mortar has an intrinsic strength of 232 MPa (34,000 psi) regardless of age or w/c shown in Figure 3 (Powers et al. 1958). Furthermore, they found a relationship that showed compressive strength increases as porosity decreases. The question may be asked why the compressive strength of conventional concrete is an order of magnitude less than the intrinsic strength of the corresponding portland cement mortar. The answer is found in understanding the interfacial transition zone (ITZ) of concrete and will be discussed in the next section.

Figure 3: Strength-Porosity relationship in portland cement mortar (Powers, 1958)

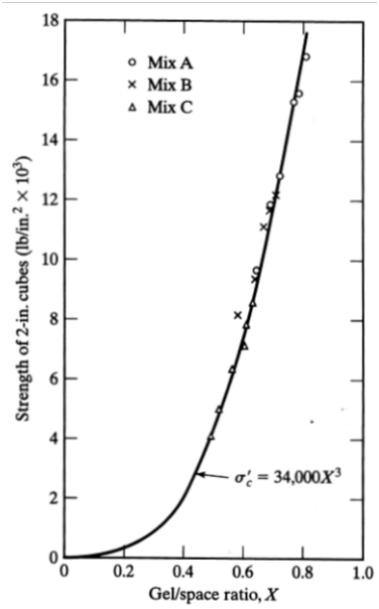

2.2.3 Interfacial Transition Zone in Concrete

Historically, concrete has been seen as having two phases, the aggregate phase and the hydrated cement phase. However, these two phases alone could not explain some properties of concrete mentioned in the earlier section such as why hydrated cement paste has a higher compressive strength than the corresponding concrete itself or why the constituent materials of concrete behave more elastic before fracture whereas the concrete itself behaves inelastic. The ITZ is commonly referred to the area between the aggregate and the hydrated cement paste. While the ITZ itself is made of the same products as the bulk hydrated cement paste there are some differences in the microstructure and behavior of hydration products at this area. Maso describes the ITZ as having the following characteristics (Maso, 1980). First, the w/c ratio is higher around the aggregates than away from it due to a film of water that tends to form around the aggregate. Second, the platelike

and weaker CH crystals serve as a preferred cleavage site due to its tendency to congregate around the aggregate and orient itself perpendicular to the aggregate surface. When the material is stressed, the ITZ is the source of initial cracks which occurs throughout the concrete matrix. When these cracks become continuous and connect with each other, the material fails in a brittle behavior. Figure 4 illustrates the preferred orientation of CH around the aggregate and the reduced amount of C-S-H at the transition zone compared to the bulk cement paste.

Figure 4: Three phases of concrete (Folliard, 2015)

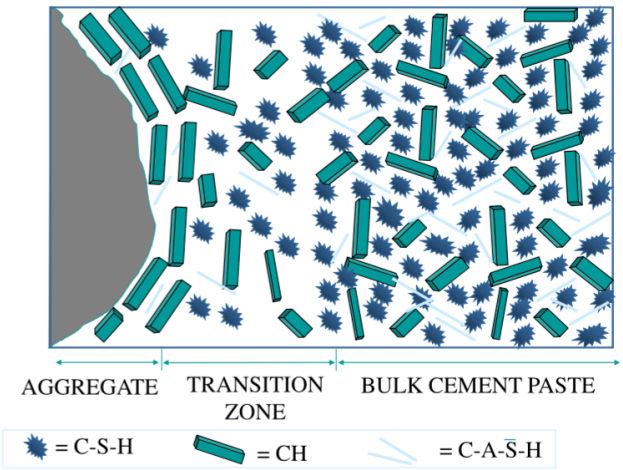

The ITZ is described as the strength limiting phase in concrete and explains the disparity between the strength of hydrated cement paste and the corresponding concrete material. Mehta points out that the characteristics of the ITZ described by Maso makes the material susceptible to cracking due to differential movement between the aggregate and hydrated cement paste leading to tensile stresses. The differential movement commonly occurs during drying or cooling which means a concrete can have microcracks in the transition zone even before loading (Mehta and Monteiro, 2014). When stressed, these microcracks that are already present in the transition zone can easily extend itself before

failure which explains why concrete behaves inelastic before failure. The concrete is set up to fail even before applying stresses to it. In order to optimize the strength of the material, the ITZ is a critical component that needs careful consideration.

As with the rest of the bulk cement paste, age helps to strengthen and densify the transition zone, but the most effective way of dealing with the ITZ is with the use of supplementary cementitious materials (SCMs). Overall, SCMs disrupt the preferred orientation of CH and also promotes the formation C-S-H to help densify and strengthen the transition zone. The benefits of SCMS such as silica fume will be discussed in detail at a later section.

2.3 Materials and Mixture Properties

While each UHPC mix may differ, there are similarities that help it achieve the desired properties. In the 2016 FHWA report, Graybeal detailed a typical UHPC composition, shown in Table 1. There are some unique elements to this mix design that can generally be applied to other UHPC mixes and are not normally seen in conventional concrete. First, UHPC mixes have a very low water to cement ratio and in some cases as low as 0.15. Second, the amount of silica fume used is higher than normal upwards of 25% replacement of cement. Next, the amount of steel fibers used equates to roughly 2% by volume. Lastly, a typical UHPC mix does not contain coarse aggregates. This next section describes in more detail typical elements that may be found in a UHPC mix.

Table 1: Typical UHPC composition (Graybeal, 2006)

Material	**Amount ($kg/m^3 (lb/yd^3)$)**	**Percent by Weight**
Portland Cement	712 (1,200)	28.5
Fine Sand	1020 (1,720)	40.8
Silica Fume	231(390)	9.3
Ground Quartz	211(355)	8.4
Superplasticizer	30.7(51.8)	1.2
Accelerator	30.0 (50.5)	1.2
Steel Fibers	156(263)	6.2
Water	109(184)	4.4

2.3.1 Dry Constituents

Due to the absence of coarse aggregates, the largest granular material found in the mix is the fine sand. The next largest particle is the cement at an average diameter of 15μm (Kosmatka et al. 2011). In some cases, the mix may also contain crushed quartz with an average diameter of 10μm (Graybeal, 2006). The smallest material is the silica fume with an average diameter of 0.1 μm (Kosmatka et al. 2011). The choice of materials is intentional in order to optimize the mix across the entire size spectrum to pack and densify as much material as possible. The largest material in a typical UHPC mix are the steel fibers. The type of steel fibers used in the proprietary mix and in this study, have properties shown in Table 2.

Table 2: Steel fiber properties

Length	13 mm (0.5 in)
Diameter	0.2 mm (.0079 in)
Tensile Strength	2,160 N/mm^2(313 ksi)
Young's Modulus (E)	210,00 N/mm^2 (30,450 ksi)
Specific Gravity	7.85
Aspect Ratio	63.3

2.3.2 Characteristics of Silica Fume

Silica Fume is a by-product from the production of silicon, ferro-silicon, and other silicon alloys. ASTM C 1240, *Silica Fume Used in Cementitious Mixtures* is the standard governing the use of the material. The chemical requirements for silica fume is shown in Table 3. In addition to these chemical requirements, some typical characteristics of silica fume include a very amorphous (glassy) structure which makes it a highly reactive pozzolan. In addition, silica fume tends to have a specific surface area > $15000\ m^2/kg$ compared to cement with a specific surface area ~ $350\ m^2/kg$. Silica fume also has a spherical particle shape and is roughly 0.1 μm in diameter. The characteristics of silica fume affect the following properties of fresh concrete shown in Table 4. Due to the fine particle size, silica fume reduces the workability of the mix and also requires more water. These implications are particularly important when dealing with UHPC due to the need for the material to be self-leveling and the already low w/cm of UHPC mixes.

Table 3: Silica fume chemical requirements (ASTM C 1240)

$SiO_2, min, \%$	85.0
Moisture content, max, %	3.0
Loss on ignition, max, %	6.0

Table 4: Impact of silica fume on fresh concrete properties

Water demand	Increases
Workability	Decreases
Bleeding and segregation	Decreases
Setting time	No impact
Air content	Decreases
Heat of hydration	No impact

The benefits of silica fume include 1) its role in the micro-filler effect, 2) the "wall effect", 3) the pozzolanic reaction, and 4) the pore blocking effect, all of which help to increase strength and reduce permeability.

1) **Micro-filler effect –** Due to the size of silica fume ($1/100^{th}$ the average size of a cement grain), the particles are able to fill the space in between cement grains. For a mix with 15% replacement of silica fume, this equates to about 2,000,000 particles of silica fume for each grain of cement (Folliard, 2015). Having silica fume allows a densified mix and also minimizes porosity. The micro-filler effect is shown in Figure 5.

Figure 5: Micro-filler effect of silica fume (Folliard, 2015)

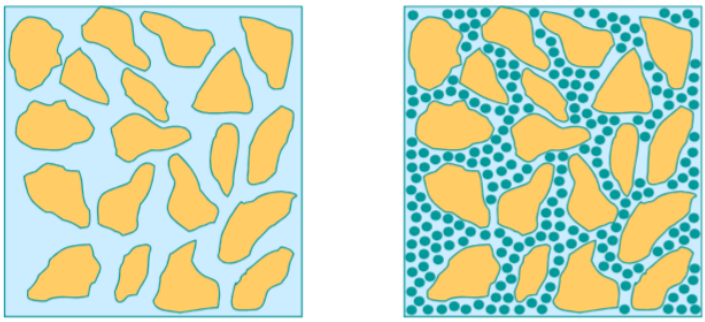

2) **Wall-Effect –** The wall effect can be explained with a jar of marbles. The marbles are unable to pack itself at the wall of the jar as well as the area away from the jar. Similarly, cement grains pack better away from the aggregate than next to it. As discussed in an earlier section, the cement aggregate interface also known as the ITZ is a source of weakness in concrete. Silica fume densifies the transition zone and also increases bonding between the aggregate and hydrated cement paste shown in Figure 6.

Figure 6: Benefit of silica fume on wall effect (Folliard, 2015)

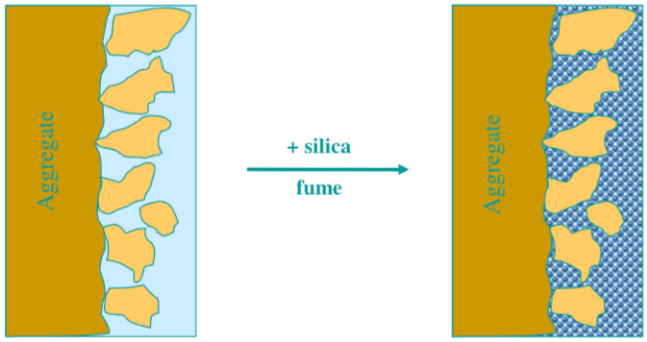

3) **Pozzolanic reaction** – Arguably the greatest benefit of silica fume is its pozzolanic nature. ACI definies a pozzolan as a siliceous or silico-aluminous material that, in finely divided form and in the presence of moisture, chemically react with calcium

hydroxide at ordinary temperatures to form compounds having cementitious properties (ACI, 2013). In simpler terms, pozzolans react with weaker CH products to form stronger C-S-H products. It is known that when calcium silicates from Portland cement react with water, both C-S-H and CH is formed shown with the reactions below.

$$2C_3S + 6H \rightarrow C_3S_2H_3 + 3CH$$
$$2C_2S + 3H \rightarrow C_3S_2H_3 + CH$$

In the presence of silica fume, the CH reacts with the silica fume to form C-S-H shown in the reaction below. The formation of more C-S-H is overall beneficial to the mechanical and durability properties of the concrete.

$$xCH + yS + zH \rightarrow C_xS_yH_{x+z}$$

4) **Pore blocking effect –** As discussed in a previous section, C-S-H forms in and around the cement grain whereas weaker and porous CH products form in the space away from the cement grain. As a result, these areas in between cement grains act as a weaker and porous location for the hydrated cement paste. The use of silica fume not only increases the amount of C-S-H, but also reacts with CH to form C-S-H in the space away from the cement grain. This is known as the pore blocking effect shown in Figure 7. This also benefits the concrete microstructure by decreasing the porosity and promoting a disconnected pore structure also known as percolation.

Figure 7: Pore blocking effect of silica fume (Folliard, 2015)

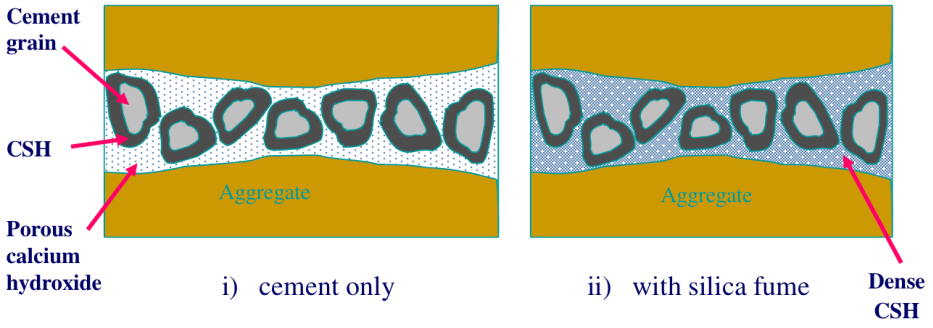

2.3.3 Characteristics of Fiber-Reinforced Concrete

Fibers are added to concrete to improve the strength, toughness, fatigue, impact and cracking properties. The application determines the aggregate size, fiber type and fiber geometry. For example, low amounts of fibers (< 0.5-1% by volume) are typically used to control shrinkage cracking. For applications using UHPC, steel fibers are the most common fibers used at 2% by volume. In these cases, the main benefits for using fibers is in its toughness properties.

2.3.3.1 Toughness Benefits of Fiber Reinforced Concrete

Toughness is a measure of the energy required to fracture the material represented by the area under the stress strain curve. In general, fiber reinforced concrete (FRC) and unreinforced concrete behave similarly and linearly until first crack. Figure 8 shows a comparison of the tensile behavior of unreinforced and fiber reinforced concrete (Mehta and Monteiro, 2014). For normal unreinforced concrete, the material has no load-carrying capacity past initial crack and fails in a brittle manner. When adding fibers, there are two responses the concrete may experience depending on the amount and type of fibers used. If the post cracking strength, σ_{pc}, is less than the cracking strength, σ_{cc}, only one crack

forms followed by a gradual loss of load as the specimen elongates due to fiber pull out (Figure 8). The second possible response is a strain hardening behavior common in strain hardening cementitious concrete (SHCC) which UHPC falls under. As opposed to normal fiber reinforced concrete, strain hardening behavior is achieved by the formation of multiple cracks vs a single cracking opening. This is achieved when the post cracking strength is greater than the cracking strength of the material ($\sigma_{pc} > \sigma_{cc}$). As the material continues to be stressed, individual cracks form and begin engaging the fibers. When the collective fibers bridging cracks reach an ultimate pullout resistance, the post cracking strength is reached and the stress gradually decreases (Figure 8). Compared to unreinforced concrete, SHCC is able to take a load past initial crack while the material continues to elongate.

Figure 8: Tensile behavior of plain and fiber reinforced concrete (Mehta and Monteiro, 2014)

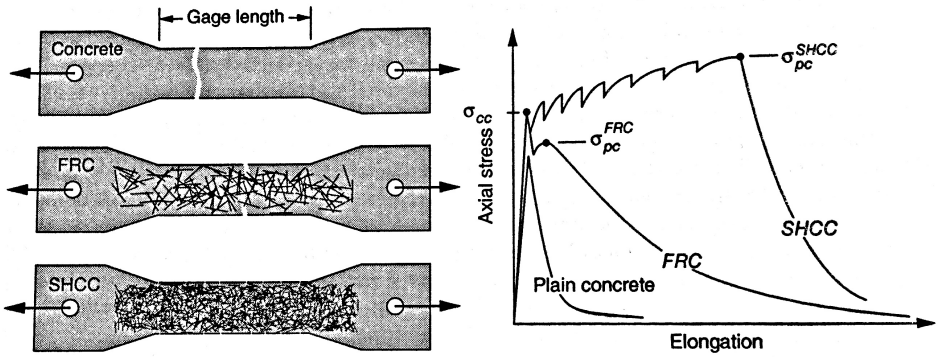

2.3.3.2 Fiber Pullout

An important component of achieving strain hardening behavior is in allowing the fibers to pull out before they fracture. This is done by paying attention to the interaction between the hydrated cement paste, aggregates, and the fiber itself. Factors that affect this

interaction include the shape and texture of the fibers. When allowed to pull out, the fibers are able to carry the load across multiple cracks in the concrete as shown in Figure 8. The small drops in load shown for SHCC are indicative of the individual cracks forming and fibers being engaged. This would not be possible if the fiber's fracture strength was less than its ability to resist pull out. In comparison to normal unreinforced concrete, the total energy absorbed in fiber debonding was found to be 10 to 40 times higher in SHCC (ACI Committee 554). This is a comparably large difference leading to its superior tensile and post cracking behavior.

2.3.3.3 Durability with Fibers

In addition to the benefits to toughness, SHCC has improved performance in durability. The multiple fine cracks formed keep the matrix tight and slows down the movement of water transporting any detrimental ions into the concrete as opposed to a single larger crack. Initially, the use of steel fibers led to a concern with corrosion of the steel fibers. While surface staining may occur, corrosion of the steel fibers within the matrix is not a concern. In order for corrosion to occur, the following requirements must all be met: 1) galvanic couple, 2) electrical circuit, 3) moisture, and 4) oxygen (Thomas, 2015). All of these elements are met in concrete reinforced with steel fibers with the exception of number two, an electrical circuit. During mixing, the steel fibers are dispersed and kept discontinuous throughout the matrix. Therefore, because the steel fibers are generally not in contact with one another, the matrix is unable to create a continuous electric circuit.

2.3.3.4 Workability of Fiber Reinforced Concrete

The use of fibers has widely been known to reduce the workability of fresh concrete. The two main variables effecting workability are aspect ratio and the amount of

fibers used. While these two factors decrease workability, increasing these two variables does in fact increase the toughness and strength of the concrete. The application will govern the balance of these two variables when considering workability. In terms of aspect ratio, past research has shown aspect ratios above 100 should not be used to avoid the phenomenon called curling up (Swamy et al. 1974). The optimized amount of steel fibers commonly used is around 2% by volume.

Another factor impacting the workability of fiber reinforced concrete is the size of aggregates used. Larger aggregates have an adverse effect on the workability of fiber reinforced concrete. The general rule is to not use aggregates larger than 19 mm (ACI, 1984). The advent of chemical admixtures such as super plasticizers have made it possible to increase the workability and even achieve self-leveling properties of fiber reinforced concrete without compromising the strength or toughness properties. The next section will describe typical chemical admixtures used for fiber reinforced concrete.

2.4 CHEMICAL ADMIXTURES

Chemical admixtures are often used to enhance a specific property of the concrete such as workability or set time. The use of water reducers helps improve placing, flow, slump, finish ability and improves surface preparation. The governing standard for chemical admixtures is ASTM C 494 *Standard Specification for Chemical Admixtures for Concrete*. Each chemical admixture is classified under the types shown in Table 5.

Table 5: Chemical admixture types (ASTM C 494)

Type A	Water reducing admixtures
Type B	Retarding admixtures
Type C	Accelerating admixtures
Type D	Water-reducing and retarding admixtures
Type E	Water-reducing and accelerating admixtures
Type F	Water-reducing, high range admixtures
Type G	Water-reducing, high range, and retarding admixtures
Type S	Specific performance admixtures

Accelerators and retarders affect the set time of the fresh concrete. Water reducers reduce the amount of water without changing the flow of the material whereas a plasticizer increases the flow without having to add more water. Water reducers can be classified under a normal conventional water reducing admixture (WRA), mid-range water reducing admixture, and high range water reducing admixture (HRWR) also known as superplasticizers.

2.4.1 High Range Water Reducer Mechanisms

Each classification has similar but different mechanisms in achieving the water reducing properties. Since most UHPC mixes use polycarboxylate HRWR's, the mechanisms for normal WRA and mid-range water reducers will not be discussed in this report. The two main mechanisms for polycarboxylate HRWR's are steric hindrance and electrostatic repulsion (Folliard, 2015). During mixing, the grains of cement tend to conglomerate with each other due the attraction of electrical charges on the surface of the cement grain. This causes the water to be tied up and not allow the cement grains to be fully lubricated reducing the workability and initial hydration.

Polycarboxylates have a polar chain carrying negative functional groups and hydrophilic side chains (Figure 9). The polar chains attach itself to the positive charges of the cement grain and surround the cement grain. During steric hindrance, the side chains physically keeps the cement grains away from one another allowing the cement grains to be completely surrounded with water. In addition, the negatively charged functional groups repel each other in what is known as electrostatic repulsion. All of this helps the fresh concrete become more fluid to improve workability of the mix.

Figure 9: Polycarboxylate polar chains and mechanisms (Folliard, 2015)

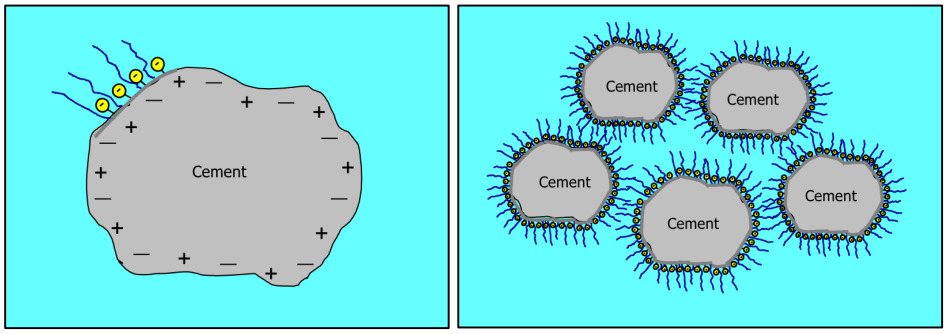

2.4.2 Accelerator and Retarder Mechanisms

In addition to water reducers, accelerators and retarders may be used to complement a UHPC mix. During early hydration, cement grains forms a diffusion barrier that controls the set time of the concrete. Both accelerators and retarders work to either weaken or strengthen this diffusion barrier to affect the set time (Kosmatka et al. 2011).

Accelerators work by weakening the diffusion barrier formed during early hydration. The most commonly used accelerators are calcium chloride (CaCl) based. CaCl breaks down the diffusion barrier and promotes the hydration of the cement grain to accelerate set time. Benefits of accelerators include accelerating the rate of hydration (set time) and early-age strength development.

In contrast, retarders work to strengthen the diffusion barrier instead of weakening them. The most common retarders contain lignosulphates that slows down the dissolution of calcium from anyhydrous cement grains and in turn slows down the formation of hydration products such as C-S-H. Retarders can be used in the following applications; 1) to offset the effects of hot weather placement, 2) delay initial set to allow more time for placement, and 3) finishing techniques for exposed aggregate surfaces.

2.5 Fresh and Hardened Properties

As discussed earlier, a thorough material characterization of UHPC was done by Graybeal for the FHWA in 2006. For completion and comparison, Graybeal provided a manufacturer supplied data sheet with typical ranges for UHPC shown below. This next section summarizes some of the findings from Graybeal's research regarding the same UHPC proprietary mix also being looked at in this report.

Table 6: Manufacturer-supplied material data sheet (Graybeal, 2006)

Material Characteristic	Range
Compressive Strength (MPa)	180-225
Modulus of Elasticity (GPa)	55-58.5
Flexural Strength (MPa)	40-50
Chloride Ion Diffusion (m^2/s)	1.9 x 10^{-14}
Carbonation Penetration Depth (mm)	<0.5
Freeze-Thaw Resistance (RDM)	100%
Salt-Scaling Resistnace (kg/m^2)	<0.012
Entrapped Air Content	2-4%
Post-Cure Shrinkage (microstrain)	0
Creep Coefficient	0.2-0.5
Density (kg/m^3)	2,440-2,550

2.5.1 Air and Unit Weight

An air void analysis was performed by Graybeal following the modified point count method from ASTM C 457 *Standard Test Method for Microscopical Determination of Parameters of the Air Void System in Hardened Concrete*. The research looked at the effect of the location of cylinders, the amount of time on the vibrating table, mix stiffness, and the use of accelerator on air content. Due to the material not having any coarse aggregates, the steel fibers were counted as coarse aggregate for the experiment. Also, when comparing the stiffness of the mix, Graybeal looked at the flow where a stiff mixed had a flow of 6.5 inches and a normal mix had a flow of 7.5 inches. Overall, the air content for the different testing conditions fell around 6.5% (Graybeal, 2006). Some trends that were noticed include air content being more at the bottom of the cylinder as opposed to the surface of

the cylinder. This may be due to the air escaping out of the top from vibration. Also, placing the cylinders on a vibrating table longer led to a decrease in air content. When comparing consistency of the mixes, the stiffer mix tended to have less air than a normal flow mix. Lastly, there were no definitive differences in air content when using accelerators.

The density of the material was determined with the individual cylinders that were casted. These results were based on four different curing methods, steam treated, untreated, tempered steam treated and delayed steam treated. Based on the tests, the density of UHPC ranged from 2,400 to 2,500 kg/m^3 (150 to 156 lb/ft^3 regardless of curing method (Graybeal, 2006). The steam treated method meant steaming the UHPC at 194 °F and 95% relative humidity for 48 hours. This included 2 hours of increasing steam and 2 hours of decreasing steam. The untreated curing method involved keeping the specimens in a standard laboratory environment until testing. The tempered steam method was similar to the steam treatment but at a temperature of 140 °F. Lastly, the delayed treatment is the same as the steam treatment but delaying steam curing until the 15th day.

2.5.2 Slump and Rheology

The slump of UHPC is governed by the individual material constituents. As discussed previously, the workability of UHPC is low due to the use of silica fume and fibers. In order to improve workability, HRWR's are used to achieve self-leveling properties. Due to the effects of fibers, the slump cone test is not recommended for concrete with fibers. While fibers may reduce the measured slump, the placeability and compactibility of the fresh concrete may still be acceptable for field casting applications (Mehta and Monteiro, 2014). Instead, the Vebe test or ASTM C 1437 *Standard Test Method for Flow of Hydraulic Cement Mortar* is recommended.

The Vebe test was developed by Swedish engineer V. Bährner. The test measures the amount of time reported in Vebe seconds it takes to remold a fresh concrete sample shaped from a typical slump cone into a leveled cylindrical shape when placed on a vibrating table.

Graybeal focused entirely on a modified version of the ASTM C 1437 flow test. Instead of using the ASTM specified caliper recommended in the test and reporting the flow as a percentage of the base diameter, the widths of the samples were taken before and after the 20 tamping blows were applied. The study found the values ranged from 165 to 210 mm (6.5 to 8.25 inches) (Graybeal, 2006). A flow reading of 8 inches and above is considered to be adequate for placement of UHPC.

2.5.3 Set Time

Initial and final set times were determined using penetration resistance testing following AASHTO T197. Per the standard, initial set is defined when the material reached a penetration resistance of 3.4 MPa (500 psi). Final set is defined when the material reaches a penetration resistance of 27.6 MPa (4,000 psi). Graybeal found UHPC to not start setting until at least 12 hours after casting. In general, for the UHPC tested, initial set occurred around 15 hours whereas final set occurred not too long afterwards around 17 hours after casting (Table 7).

Table 7: Set time of UHPC (Graybeal, 2006)

Curing Regime	**Initial Set (hours)**	**Final Set (hours)**
Steam	15.25	18 to 20
Untreated	Less than 14.5	16
Tempered Steam	Less than 15	15.75
Delayed Steam	Between 9.5 and 17.5	Between 9.5 and 17.5

2.5.4 Mechanical Properties

A considerable amount of the FHWA report focused on mechanical properties of UHPC. Mechanical properties are important because they indicate the material's ability to resist stress up to a point of failure. The next sections go over some of the tests that this research project also performed for comparison to the FHWA report. The data shown in the next sections were converted from the metric system used by Graybeal to U.S standard units. In addition to these tests, the FHWA also focused on fracture testing, shrinkage testing, creep testing, coefficient of thermal expansion, and heat of hydration.

2.5.4.1 Compressive Strength

The strength of concrete is at the core of the design of structures made of concrete. The most widely accepted test for concrete strength is the compressive strength test. The standard for the compressive strength test is ASTM C 39 *Standard Test Method for Compressive Strength of Cylindrical Concrete Specimens*. Uniaxial compression tests are the most commonly used tests because of the ease of running the test. In addition, the 28-day strength test is a general index for the strength of concrete and is commonly used in field applications.

The compression tests were performed primarily on 3 inch by 6 inch cylinders. Each mold was placed and filled to the top with scoops on top of a vibrating table.

Afterwards, the molds were kept on top of the vibrating table for a few extra seconds and the tops were screeded. The molds were not rodded due to the presence of fibers.

The surface preparation of UHPC is more involved than conventional concrete due to the high strength and presence of fibers. For the FHWA report, the planeness of the cylinders was ensured with the use of an end grinder. All cylinders that were expected to have a compressive strength below 83 MPa (12 ksi) was sulfur capped. This was done to ensure fibers would not pull out from end grinding due to the weaker strengths. However, Graybeal also ran tests to measure the impact of out of planeness of the cylinders on compressive strength. Of about 250 cylinders tested for compressive under the four different curing regimes, Graybeal found the out of planeness of the cylinders to have little impact on the compressive strength (Graybeal, 2006). This could be due to the compression machine having a spherical bearing to accommodate for the differences in planeness.

Another common practice for UHPC is to increase the load rate from the recommended standard to 150 psi/sec. Graybeal and Weldon both found increasing the load rate had little to no effect on the compressive strength (Graybeal, 2006 and Weldon et al. 2012). The reasoning behind this decision is to decrease the amount of time it takes to run the test. With the high compressive strengths of UHPC, a single test can take up to 20 minutes to run.

2.5.4.2 Effect of Fibers on Compressive Strength

A study by Shah and Rangan looked at the impact of fibers on the compressive strength of concrete. They concluded that while fibers do increase the strength of concrete, the effect of fibers on toughness is more pronounced (Shah et al. 1971). Table 8 shows the results of the tests done by Shah and Rangan on a concrete mix with 1% of fibers by volume. Based on the results, fibers can have as much as a 10-fold increases in relative

toughness whereas the relative strength increases by less than 2 times the value of unreinforced concrete. In addition, the study found that increasing the aspect ratio also increases both the toughness and strength although as it was discussed earlier, this also has an adverse effect on workability. Also, worth noting is the type of failure fiber reinforced concrete exhibits. Conventional concrete is brittle and at higher strengths fails dramatically. In comparison, concrete with fibers do not fail as dramatic during failure and only exhibiting a drop in load rate. This is due to the fibers having a restraining and confining effect keeping the specimen shape intact.

Table 8: Effect of fibers on compressive strength (Shah et al. 1971)

Type Reinforcement	**Aspect Ratio L/d**	**Relative Strength**	**Relative Toughness**
Plain concrete	0	1.0	1.0
Fibers	25	1.5	2.0
Fibers	50	1.6	8.0
Fibers	75	1.7	10.5
Fibers	100	1.5	8.5

2.5.4.3 Effect of Specimen Geometry on Compressive Strength

The most common specimen geometry for testing compressive strength in the United States is the cylinder, whereas the cube is the most common specimen geometry in Europe. In general, cubes are known to have a higher strength compared to cylinders due to the shorter aspect ratio. Graybeal compared the strengths of cylinders and cubes at 28 days without any special curing shown in Table 9. The results from this study found the compressive strengths for five different specimen geometries not varying more than 8% from the control. The reason behind using cubes versus cylinders is to ensure the planeness

of the specimen. Cube molds are typically made of steel and are able to ensure the planeness of five of the six sides.

Table 9: Effect of specimen geometry on compressive strength (Graybeal, 2006)

Specimen Geometry	**Compressive Strength (psi)**	**% Difference from Control**
3 inch cylinder	21610	-
4 inch cylinder	22340	3.7
2 inch cylinder	20310	-5.9
4 inch cube	23350	8.0
2 inch cube	22920	6.1

2.5.4.4 Compressive Strength Gain of UHPC

Compressive strength of UHPC has a rapid strength gain in early ages shown in Table 10 (Graybeal, 2006). The immediate effects of the silica fume are shown due to the micro filler effect. The strength gain begins to plateau early on and the rate of strength gain decreases more over time with little strength gain between 28 and 57 days. The data also shows UHPC can reach strengths upwards of 24 ksi in only three days when steam cured versus 10.5 ksi in the same amount of time. This may be useful for precast plants that employ steam curing of their precast members.

Table 10: Compressive strength gain of UHPC (Graybeal, 2006)

Age (days)	**Steam Compressive Strength (psi)**	**Untreated Compressive Strength (psi)**
1	1100	2180
3	24510	10590
7	-	12910
15/14	25960	15950
28	26110	17260
56/57	26980	18130

2.5.4.5 Tensile Strength

The brittle nature of concrete is due primarily to the behavior of concrete in tension. Currently, there are no standard test methods to accurately test the tensile strength of concrete. There have been direct tension tests developed although the material tends to fail at the connection and not accurately measure the tensile strength. The most common method to measure tensile strength of concrete is the splitting tensile test. Compared to other tensile tests, the splitting tensile test is the simplest test to perform. The standard for the splitting tensile test is ASTM C 496 *Standard Test Method for Splitting Tensile Strength of Cylindrical Concrete specimens*. The test measures the tensile strength by applying a compressive load on a cylinder placed on its side. The compressive stress produces a transverse tensile stress that creates a vertical crack on the specimen.

The tensile strength has been found to be related to the compressive strength although not directly. In general, the tensile strength of concrete increases at a lower rate than the compressive strength. Also, the relationship with compressive strength is different depending on the type of concrete and age. A study from students at the University of

California at Berkeley found the tensile to compressive strength ratio around 10-11% for low strength concrete, 8-9% for moderate strength concrete and 7% for high strength concrete (Mehta and Monteiro, 2014).

2.5.4.6 Tensile Strength of UHPC

The FHWA subjected the UHPC in four different tests to include the splitting tensile test measured previous, ASTM *Standard Test Method for Flexural Toughness and First-Crack Strength of Fiber-Reinforced Concrete (Using Beam with Third Point Loading)*, AASHTO T132 *Standard Method of Test for Tensile Strength of Hydraulic Cement Mortars,* and a direct tension test developed by Graybeal using different test method standards. For comparison with this project, some of the data from the splitting tensile is shown in Table 11. As expected, the treated samples experienced a higher cracking strength and ultimate strength compared to the untreated specimens. In addition, both mixes exhibited little increase in strength from 14 days to 28 days. The data also shows the benefits of fibers allowing the specimens to carry a load past first crack. It is worth noting the ultimate splitting tensile strength may not be the most accurate test for tensile strength of UHPC. This is because the cracks that are parallel to the compressive stresses get bridged by the fibers and carry a larger load before fiber pullout. The equation for tensile strength from ASTM C 496 does not account for this behavior and may not be appropriate for the material. However, the data still the shows the benefits of fibers for tensile strength when comparing to other mixes.

A UHPC cylinder under the tensile strength test will experience a crack and then transition into a phase where the fibers are engaged. In order to monitor the first crack, Graybeal developed a set up with LVDT's to measure the lateral displacement of the cylinder shown in Figure 10. During first crack, the lateral displacement jumps and the

displacement increases less linearly as more load is applied. In addition, the study found the first crack can sometimes be audible. Graybeal found that the tensile strength reported for the splitting tensile test was in general 30% more than the direct tension tests for all curing methods.

Table 11: Splitting tensile strength of UHPC (Graybeal, 2006)

Age (days)	**Steam Cracking Strength (psi)**	**Untreated Cracking Strength (psi)**	**Steam Ultimate Strength (psi)**	**Untreated Ultimate Strength (psi)**
5	1800	960	3840	2190
14	1680	1280	3500	2810
28	1580	1330	3510	2760

Figure 10: Split-cylinder test with lateral expansion apparatus (Graybeal, 2006)

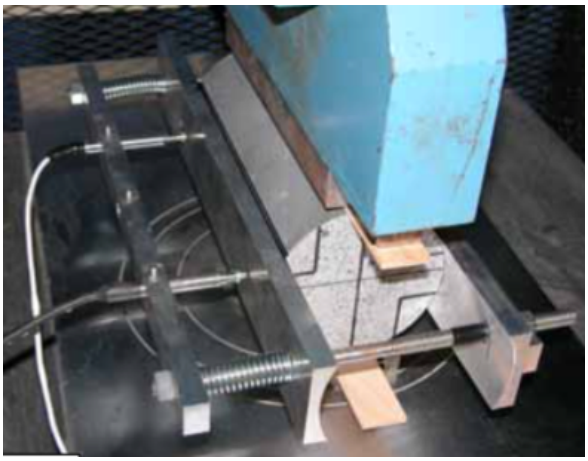

2.5.4.7 Modulus of Elasticity

The modulus of elasticity is a measure of a material's ability to resist deformation under an applied load. The standard for determining modulus of elasticity is ASTM C 469 *Standard Test Method for Static Modulus of Elasticity and Poisson's Ratio of Concrete in*

Compression. It is worth noting that fibers are expected to have only little effect on the modulus of elasticity of concrete (Mehta and Monteiro, 2014). This is partly due to the amount of fibers used (typically less than 2% by volume) compared to the bulk of the concrete.

Some factors affecting the modulus of elasticity include density, aggregate type and quantity, the cement paste matrix, and the transition zone (Mehta and Monteiro, 2014). The density of a material is related to the porosity of the material. Intuitively, a dense material correlates to a material with less porosity. Therefore, the same factors that affect the porosity of a material as discussed in the earlier sections also affect the density. Aggregates play a part in the modulus of elasticity because a dense aggregate typically leads to a higher modulus of elasticity for the concrete. In contrast, lightweight and porous aggregates have a lower modulus of elasticity and those properties are translated to the concrete modulus of elasticity. The cement paste matrix plays a role because of the amount of hydration products formed compared to the porosity. As a reminder, the formation of more hydration products through curing, SCM's, and a lower water to cement ratio promotes a mix matrix with less porosity and thus more density. Lastly, the transition zone again plays a large factor in the modulus of elasticity of concrete. As mentioned previously, the transition zone is a weak area of the concrete due to the high water to cement ratio, the preferred orientation of the more porous CH products and the micro cracks that form even before loading. The microcracks at the transition zone are spots that can exhibit a strain even before fracture leading to a lower modulus of elasticity. All these factors affect the porosity of the concrete and thus also affects the density.

2.5.4.8 Effect of Microcracks on the Modulus of Elasticity

The progressive microcracking of cracking under and applied load was first researched by Hsu et al. in 1971. In this study, microcracking of concrete was divided into four stages. During the first stage below 30% of the ultimate stress, the microcracks at the transition zone are considered stable and the stress strain curve is linear. At the next stage above 30%, the microcracks begin to increase in length, width and number. During stage two, the microcracks are considered stable up to 50% of the ultimate strength. Above 50% of the ultimate strength, the microcracks develop into cracks in the concrete matrix causing the stress strain curve to become less linear moving toward horizontal. At the fourth and final stage, above 75% of the ultimate strength, the strain increases to the point where the cracks become continuous and the concrete fails.

Because of this phenomenon, the ASTM standard for compressive strength allows a higher rate of loading up to 50% of the ultimate strength due the microcracking being in a stable condition. In addition, this also explain why the standard for modulus of elasticity requires the specimen to be taken to only 40% of the ultimate strength. This is to keep the specimen within the stable zone for microcracking. It is also worth noting that although 40% of the ultimate strength is within the stable zone for microcracking, it is outside what is considered by Hsu to be the linear zone at 30% of the ultimate strength.

2.5.4.9 Rate of Elastic Modulus Development for UHPC

The modulus of elasticity is closely related to the compressive strength and typically gains in age similarly. However, it is possible for the ITZ to become strengthened and densified over a long period time causing the modulus of elasticity to increase at a faster rate than compressive strength up to a year later.

Table 12 shows data from Graybeal looking at the modulus of elasticity of UHPC for both steamed and untreated concrete. Similar to compressive strength, the rate of

modulus of elasticity gain was larger for the first week and began to plateau afterwards with very little change in value. Also, the steam curing UHPC achieved a higher modulus of elasticity of 7,590 ksi in 28 days versus 6,080 ksi for the untreated UHPC. These numbers are indicative of the optimized gradation of the proprietary UHPC mix filling in the spaces of concrete resulting in a mix with greater density compared to conventional concrete.

Table 12: Modulus of elasticity of UHPC (Graybeal, 2006)

Age (days)	**Steam Modulus of Elasticity (ksi)**	**Untreated Modulus of Elasticity (ksi)**
1	1100	1520
3	7470	5220
7	-	5660
15/14	7570	5980
28	7590	6080
56/57	7610	6090

2.5.4.10 Toughness of UHPC

The greatest benefit of fibers can be found in the toughness of the material. The benefits of fibers in toughness were discussed in an earlier section and should be reviewed if necessary. There are currently two standards to measure the benefits of fibers in concrete. The first is ASTM C 1399 *Standard Test Method for Obtaining Average Residual Strength of Fiber-Reinforced Concrete* and the second is ASTM C 1609 *Standard Test Method for Flexural Performance of Fiber-Reinforced Concrete (Using Beam with Third-Point Loading)*. Both tests are similar in setup although ASTM C 1609 is a closed loop test. The

FHWA report tested UHPC using ASTM C 1018 which was a precursor to ASTM C 1609. ASTM C 1018 is no longer in publication although ASTM C 1609 for the most part is the same test. This ongoing research project opted to study the effect of UHPC using ASTM C 1399 for average residual strength which the FHWA has no data for comparison. In general, the fibers showed an increase of toughness upwards of 20 times the value of plain concrete.

2.6 Durability and Long Term Performance

Due to the microstructure of UHPC, the durability is expected to be exceptional. A significant factor in ensuring a durable material is in preventing ions such as chlorides from penetrating the concrete. This is achieved through a tight, disconnected pore structure and reduced porosity. The materials present in UHPC all promote a durable microstructure described in earlier sections. To confirm the durability of UHPC the FHWA report conducted the following tests.

- ASTM C 1202 *Standard Test Method for Electrical Indication of Concrete's Ability to Resist Chloride Ion Penetration*
- AASHTO T259 *Resistance of Concrete to Chloride Ion Penetration*
- AASHTO T260 *Standard Method of Test for Sampling and Testing for Chloride Ion in Concrete and Concrete Raw Materials*
- ASTM C 672 *Standard Test Method for Scaling Resistance of Concrete Surfaces Exposed to Deicing Chemicals*
- ASTM C 944 *Standard Test Method for Abrasion Resistance of Concrete or Mortar Surfaces by the Rotating-Cutter Method*
- ASTM C 666 *Standard Test Method for Resistance of Concrete to Rapid Freezing and Thawing*

- ASTM C 1260 *Standard Test Method for Potential Alkali Reactivity of Aggregates (Mortar-Bar Method)*

2.6.1 Chloride Resistance of UHPC

The chloride resistance of UHPC from the FHWA report was very good with the average number of coulombs passed (in six hours) reported to be 360 for the standard-cured UHPC and less than 20 for the steam-cured UHPC at 28 days (Graybeal, 2006). These values are considered very low and negligible in ASTM C 1202. The chloride penetration test also referred to as a "ponding test" also showed favorable results with the amount of chlorides penetrating the concrete at 90 days to be extremely small.

These tests also provided an opportunity to visual inspect the corrosion of the steel fibers. While minor corrosion was observed, this was only considered to be surface staining and there was no indication the internal fibers were showing signs of corrosion.

2.6.2 Scaling and Abrasion Resistance of UHPC

Scaling is an issue related to the use of chloride based deicers in colder climate locations. There are currently different theories on the mechanism of scaling including a fairly new one developed by Valenza and Scherer called the glue spall mechanism. The following is a summary of the of the salt scaling characteristics per the glue spall mechanism (Valenza and Scherer, 2006).

1. Salt scaling damage is shown in the form of flakes take from the surface of the concrete
2. A pessimum effect exists at a concentration of 3%
3. Scaling does not occur without a liquid on the surface
4. Scaling does not occur when the temperature is above -10 C
5. Air entrainment reduces scaling

6. The salt concentration on the surface is a larger factor than the salt concentration in the pore solution
7. There is no correlation between scaling and frost action
8. The strength of the surface is a primary factor in a concrete's ability to resist scaling

During the tests by Graybeal, no specimens showed any indication of scaling and received a surface rating condition of zero based on the standard (Graybeal, 2006).

The abrasion test is important especially for road applications of UHPC. ASTM C944 tests abrasion by measuring the amount of concrete lost by applying a rotating cutter over a period of time. The FHWA study looked at the test for the different curing methods in addition to three different surface preparations. The surfaces tested were a steel cast surface, a sand blasted surface, and a grounded surface. It was observed that the curing method had a noticeable effect on the abrasion resistance performance of UHPC. The steam-cured specimens outperformed the untreated specimens by a factor of 10. In addition, it was observed that the smoother steel cast surface resisted abrasion more than the sand blasted and grounded surfaces.

2.6.3 Freezing and Thawing Resistance of UHPC

Similar to scaling, freezing and thawing is a common issue for colder climates. The constant freezing and thawing cycles of these climates causes the concrete to expand which leads to cracking and spalling. While there is no clear consensus to the mechanism of freezing and thawing, there are some generally agreed factors to freezing and thawing.

1. A critical saturation of more than 91.7% is required for freezing and thawing (Powers, 1958)

2. Freezing and thawing occurs when the spacing between pores are more than .008 inches (200 μm) also known as the critical spacing factor, $\bar{L}$ (Powers, 1958).
3. Air entrainment helps reduce freezing and thawing by reducing the spacing between pores to less than $\bar{L}$.

The results from Graybeal using ASTM C 666 found that UHPC was very resistant to deterioration from freezing and thawing. However, he did find that there may be some external factors to the untreated UHPC specimens. Normally, the prisms tested for freezing and thawing lose mass during the test and the relative dynamic modulus (RDM) value decreases as the specimen deteriorates. However, the specimens that were untreated increased in both mass and RDM possibly indicated that the specimens were taking on water and hydrating. To test this hypothesis, Graybeal tested the compressive strength of all the specimens. He found that the compressive strength of the steam cured specimens did not increase whereas the compressive strength of the untreated specimens did increase. This indicated that there is some form of hydrating occurring for the untreated specimens when running the freezing and thawing test.

2.6.4 Alkali Silica Reaction of UHPC

Alkali silica reaction (ASR) is a reaction between the alkalis in the pore solution of concrete and unstable silica present in some aggregates. The reaction forms an alkali silica gel that in the presence of water expands creating enough stresses in the concrete to induce cracking. In order for the alkali silica to occur, the following three factors must be present (Thomas and Folliard, 2007).

1. Reactive silica primarily in the aggregates
2. Sufficient alkalis in the pore solution

3. Sufficient moisture to induce expansion

Since the discovery of ASR, the following recommendations have been made to minimize the risk of ASR related expansion (Thomas and Folliard, 2007).

1. Use of non-reactive aggreagtes
2. Limiting alkali content of concrete
3. Use of supplementary cementitious materials (SCMs)
4. Use of lithium compounds

The FHWA report primarily focused on ASTM C 1260 also known as the accelerated mortar method to test ASR in UHPC. This decision was made due to the expediency of the test compared to ASTM C 1293 *Standard Test Method for Determination of Length Change of Concrete Due to Alkali-Silica Reaction*. It should be noted that the best method to test for ASR is by using larger exposure blocks (Folliard, 2015). This is due to the possibility of false negatives and false positives with some aggregates.

The ASTM C 1260 tests for UHPC showed good results with specimens having 14-day expansion values of no more than .013% and .012% for 28-day expansion values (Graybeal, 2006). The standard describes specimens with an expansion less than 0.1% as innocuous and greater than 0.2% as potentially deleterious. Based on the study using ASTM C 1260, ASR does not appear to be a factor for UHPC.

2.7 APPLICATIONS

Over the years, UHPC has been used in a variety of applications depending on the needs of the owner. The enhanced properties of the material have led to unique designs and applications that have not been possible in the past. These applications include use in public infrastructure, architecture, and security applications. While the most common use of

UHPC is in bridge structures, there have also been uses for UHPC in architectural applications.

One example of an architectural application is the Jean Bouin Stadium Façade in Paris France (Figure 11). The façade is made using a proprietary UHPC mix, similar to the type being researched in this report. The design is made of precast panels casted in a lattice pattern that would not have been possible with conventional concrete. Another architectural application is at the Museum of European and Mediterranean Civilisations (MuCEM) in Marseille, France (Figure 12). Both applications show the unique possibilities for architects when using UHPC in their designs.

Figure 11: Jean Bouin stadium facade - Paris, France

Figure 12: Museum of European and Mediterranean Civilizations

The most common application of UHPC is in the bridge structure community. While the technology has been available since the 1990's, much of the recent uses of UHPC has been in the past 5 years with some bridges being built entirely out of UHPC (EDC, 2016). An example of a bridge being made entirely of UHPC is the Jakway Park Bridge located in Buchanon County built in 2008 (Keierleber, 2010) (Figure 13). The shape of the girder is similar to a typical deck bulb tee girder but has bottom flanges on the outside of the webs to imitate the shape for the Greek symbol for pi (Figure 14). The material allows engineers to design a bridge with a shallower depth than typical across the length of the bridge. This project also implemented the use of a ready-mix concrete truck versus a high-speed pan mixer which is typically used for UHPC production.

Figure 13: Jakway Park bridge in Buchanon County, Iowa (Keierleber, 2010)

Figure 14: Jakway Park bridge pi shaped girder (Keierleber, 2010)

2.7.1 UHPC PBE Connections

At the moment, the cost of developing bridges entirely out of UHPC exceeds that of conventional concrete and much of the focus is on smaller bridge element applications. One area that is showing promise and interest for field application of UHPC is in pre-fabricated bridge element (PBE) connections for accelerated bridge construction (Culmo, 2011). The FHWA describes ABC as "bridge construction that uses innovative planning, design, materials, and construction methods in a safe and cost-effective manner to reduce the onsite construction time that occurs when building new bridges or replacing and rehabilitating existing bridges" (Culmo, 2011).

More specifically, UHPC has been used for connecting precast bridge deck slab elements together (Figure 15). To highlight the importance and potential of UHPC, the FHWA has chosen UHPC connections as 1 of 11 innovations in their *Every Day Counts* (EDC) initiative for 2016. The initiative is a state based model that identifies and rapidly deploy proven but underutilized innovations to shorten the project delivery process, enhance roadway safety, reduce congestion and improve environmental sustainability (Harman, 2016).

Figure 15: UHPC connections at I-81 bridge Syracuse, New York (Graybeal, 2014)

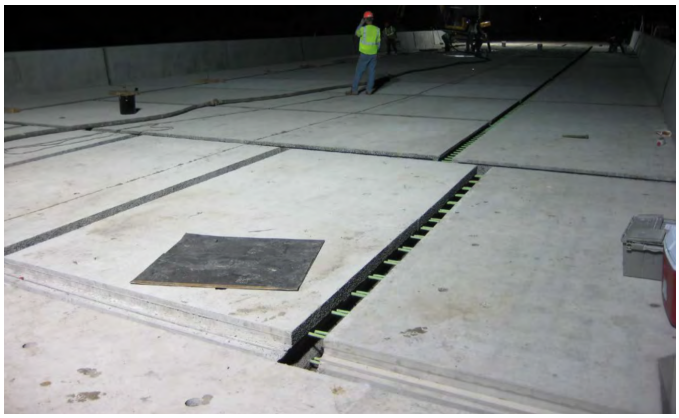

The use of UHPC allows for a stronger connection than the elements itself similar to steel design. The FHWA released a design guideline, FHWA-HRT-14-084 *Design and Construction of Field-Cast UHPC Connections* in 2014. This next section summarizes the FHWA report and will touch on some key parts. The report also looks into applications for UHPC connections for shear interfaces and substructure connections but this project only focuses on applications for bridge deck connections.

The current practice for conventional bridge deck connections has a couple options depending on the current standard of practice followed by each state department of transportation. One option is to have a closure pour with reinforced concrete which requires a wide connection up to 3'. Another option is to use a smaller connection with a specific reinforcement detail and grout. Figure 16 shows the detail of some conventional deck panel connections when using grout.

Figure 16: Conventional grout deck panel connections (Graybeal, 2016)

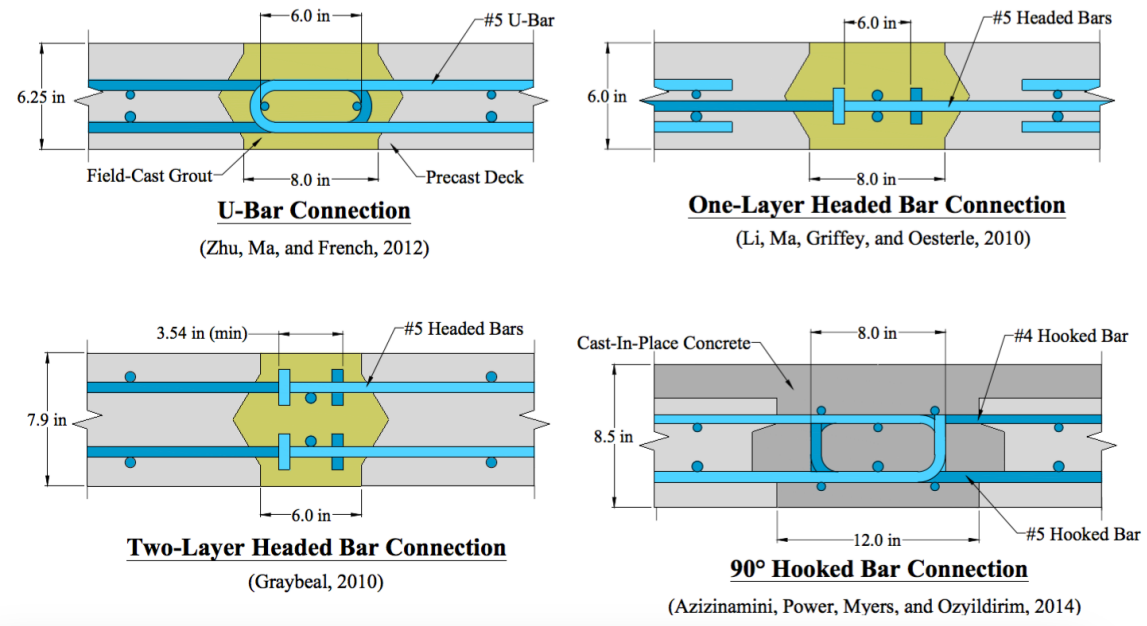

In comparison, a UHPC connection is simplified and requires a smaller connection and lap splicing of straight rebar (Figure 17). This design is possible because of the added benefits of UHPC. The EDC lists the benefits in terms of 1) Speed, 2) Simplicity, and 3) Performance (FHWA, 2016). The performance of UHPC allows for ease in construction as shown in the comparison of conventional bridge deck connections. In addition, the connections require less rebar and forgoes an involved design for a simpler one. Lastly, the mechanical performance of high compressive strength and a durable mix matrix leads to a longer lasting material. The durability is achieved with a disconnected pore structure which is beneficial in keeping water from penetrating into the concrete and transporting unwanted ions.

Figure 17: UHPC deck panel connection detail (Graybeal, 2016)

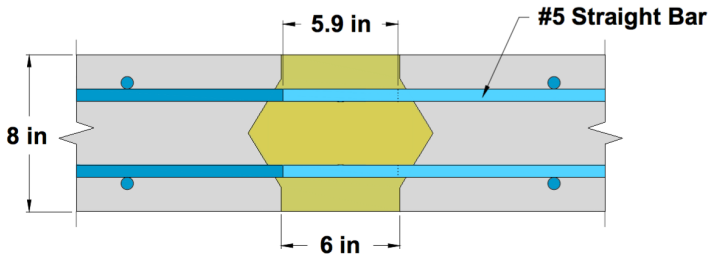

The FHWA Design Guideline for UHPC connections requires the following when using Rebar Lap Splice for deck level connections similar to Figure 17 (Graybeal, 2014):

- UHPC material
- Embedment Length, $l_d \geq 8d_b$
- Cover $\geq 3d_b$
- Bar clear spacing: between $2d_b$ and l_s
- $l_s \geq 0.75l_d$
- $f_c' \geq 14\ ksi$
- Uncoated or epoxy coated bars with up to 75 ksi yield
- No. 4 to No. 9 bar

The design guideline shows the reduced development length, as low as 5" for a #5 straight bar due to the material properties vs conventional reinforced concrete or grout when used in bridge deck connections. The report also provides guidance for different configurations such as the cover.

2.7.2 UHPC PBE Construction

When applying UHPC for bridge deck connections, there are some considerations specific to the material. First, special care needs to be shown in the construction of the forms. The rheology of the material is very fluid and tight forms are needed to prevent the

material from leaking. In order for the UHPC to have a good bond with the PBE there are some recommendations to consider. First, the connection interfaces should be wet in order to prevent the loss of moisture from the UHPC and to ensure a good bond between the PBE and the UHPC connection. Second, the surface of the PBE that is in contact with the UHPC has a retarder paste applied during casting and then washed off to achieve a rougher texture (Figure 18). This process is similar to architectural practices in achieving an exposed aggregate on the surface of a building or pavement.

Field casting of the material typically requires the use of a high-speed pan mixer in order to achieve the proper mixing on site. After mixing, the material is then poured into the connections and allowed to flow into place due to its self-leveling behavior (Figure 19). Lastly, in the case of the I-81 bridge in Syracuse, New York, the entire bridge surface was grinded in order to achieve a uniform texture across the deck.

Figure 18: Surface preparations (Graybeal, 2014)

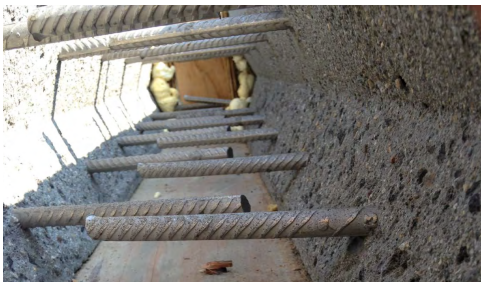

Figure 19: Field casting of connection (Graybeal, 2014)

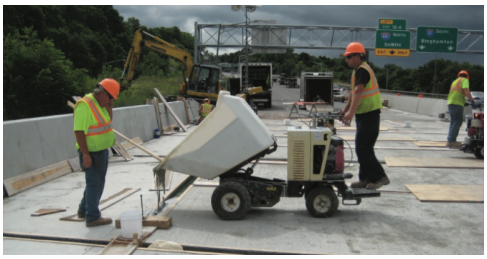

Chapter 3: Experimental Approach of Ultra High Performance Concrete

3.1 RESEARCH PLAN

This chapter describes the experimental objectives and program for this first phase of a more comprehensive effort evaluating UHPCs for transportation applications. This initial phase has two general objectives, first to verify the mechanical properties of a proprietary, premixed UHPC and second, to develop and characterize various nonproprietary mixes using local materials within the state of Texas. The tests performed on the mixes were:

- ASTM C 109 *Compressive Strength of Hydraulic Cement Mortars*
- ASTM C 469 *Static Modulus of Elasticity and Poisson's Ratio of Concrete in Compression*
- ASTM C 496 *Splitting Tensile Strength of Cylindrical Concrete Specimens*
- ASTM C 1497 *Flow of Hydraulic Cement Mortar*

The goal for the nonproprietary mix was to simulate field conditions as much as possible and to make the mixing process and placement as user friendly as possible. This included not using vibration and not applying any special heat- or steam- curing methods. Also, although UHPC is known to have high compressive strengths upwards of 30 ksi, preliminary indications from TxDOT were that significantly lower compressive strengths (e.g., 15 ksi) would suffice for the target bridge applications.

3.1.1 Batch Nomenclature

This study required close to 400 different specimens for testing. In order to keep the organization of the different mixes, a unique nomenclature was developed. Each mix has the following identifier, (U for UHPC) - (type of SCM) - (type of fiber and amount). For example, a mix with 2% steel fibers and 15% silica fume has the following

nomenclature, U-SF-S2. In addition, batches with a similar mix but a different amount of admixtures have an asterisk added to the identifier. An exception to the rule is the proprietary mix which has a designation of UD-S2.

3.1.2 Testing Matrix

As previously mentioned, the testing matrix for the study focuses primarily on compressive strength, splitting tensile strength, modulus of elasticity and average residual strength, as shown in Table 13. The batch sizes were kept constant for consistency, whenever possible. The compressive strength, tensile strength and modulus of elasticity of the material were tested at three different ages (1,7 and 28 days). Compressive strength and tensile tests included three specimens per age while modulus of elasticity had two specimens per age. Equipment is being developed and calibrated to allow for testing of residual strength following ASTM C 1399, and beams cast from each of these mixes will be tested using this method, with the findings to be incorporated into a final report to TxDOT.

Table 13: UHPC testing matrix

Batch	**Batch Description**	**Specimens Cast**	**Mix Description**	**Batch Size (ft^3)**
U-SF-S2	Compressive Strength Splitting Tensile Modulus of Elasticity	9 2x2x2 cubes 12 3x6 cylinders 6 4x4x14 beams	2% Steel Fibers 15% Silica Fume	1.28
U-SF-S2*	Compressive Strength Splitting Tensile Modulus of Elasticity	18 2x2x2 cubes 21 3x6 cylinders	2% Steel Fibers 15% Silica Fume	0.74
U-SF-S1.5	Compressive Strength Splitting Tensile Modulus of Elasticity	9 2x2x2 cubes 12 3x6 cylinders 6 4x4x14 beams	1.5% Steel Fibers 15% Silica Fume	1.28
U-SF-S1.5*	Compressive Strength Splitting Tensile Modulus of Elasticity	9 2x2x2 cubes 12 3x6 cylinders 6 4x4x14 beams	1.5% Steel Fibers 15% Silica Fume	1.28
U-SF-S1	Compressive Strength Splitting Tensile Modulus of Elasticity	9 2x2x2 cubes 12 3x6 cylinders 6 4x4x14 beams	1.0% Steel Fibers 15% Silica Fume	1.28
U-SF-P2	Compressive Strength Splitting Tensile Modulus of Elasticity	9 2x2x2 cubes 12 3x6 cylinders 6 4x4x14 beams	2.0% PVA Fibers 15% Silica Fume	1.28
U-SF-P1	Compressive Strength Splitting Tensile Modulus of Elasticity	9 2x2x2 cubes 12 3x6 cylinders 6 4x4x14 beams	1.0% PVA Fibers 15% Silica Fume	1.28
U-MK-S1**	Compressive Strength Splitting Tensile Modulus of Elasticity	9 2x2x2 cubes 12 3x6 cylinders 6 4x4x14 beams	1% Steel Fibers 22.5% Metakaolin	1.28
U-SF-0	Compressive Strength Splitting Tensile Modulus of Elasticity	9 2x2x2 cubes 12 3x6 cylinders 6 4x4x14 beams	0% Steel Fibers 15% Silica Fume	1.28
U-SF-0*	Compressive Strength Splitting Tensile Modulus of Elasticity	9 2x2x2 cubes 12 3x6 cylinders	0% Steel Fibers 15% Silica Fume	0.4
U-MK-S2	Compressive Strength Splitting Tensile Modulus of Elasticity	9 2x2x2 cubes 12 3x6 cylinders 6 4x4x14 beams	2% Steel Fibers 15% Metakaolin	1.2
UD-S2	Compressive Strength Splitting Tensile Modulus of Elasticity	9 2x2x2 cubes 12 3x6 cylinders 6 4x4x14 beams	Proprietary Mix	1.05

Table 13: UHPC testing matrix

Batch	Batch Description	Specimens Cast	Mix Description	Batch Size (ft^3)
U-MK-S1	Compressive Strength Splitting Tensile Modulus of Elasticity	9 2x2x2 cubes 12 3x6 cylinders 6 4x4x14 beams	1% Steel Fibers 15% Metakaolin	1.2

* Mixes with a modified amount of admixture
** Non-proprietary mix with 22.5% replacement of metakaolin

3.1.3 Specimen Geometry

The compressive strengths were measured using cubes cast in 2 in x 2 in x 2 in steel molds. It was decided to use cubes, based on preliminary tests that showed cylinders were too challenging to test, due to limitations in the upper bound limit of strength when using sulfur capping or neoprene pads. In addition, the steel molds provided two parallel faces to avoid needing to grind the cylinders down for planeness. The splitting tensile and modulus of elasticity specimens were casted using 3 in x 6 in single use plastic molds. In addition, plastic caps were used with the plastic molds to help retain moisture. The 3 in x 6 in sizes are typical for UHPC testing due to the high loads from UHPC and potential capacity issues with compression machines, as well as due to the lack of coarse aggregates in the mix. Both specimens are shown Figure 20 and Figure 21 below.

Figure 20: 3 in by 6 in UHPC cylinders

Figure 21: 2 in x 2 in x 2 in UHPC cubes

3.2 Material Selection for Nonproprietary UHPC

The cementitious and supplementary cementitious materials used for the nonproprietary UHPC mixes were cement, silica fume, and metakaolin. An oxide analysis of the materials was performed with the results shown in Table 14. A representative sample was taken for both the Type I/II cement and silica fume. The two metakaolin packages used are expressed as metakaolin I and metakaolin II.

Table 14: Nonproprietary UHPC material oxide analysis

Oxide *	**Type I/II Cement (%)**	**Metakaolin I (%)**	**Metakaolin II (%)**	**Silica Fume (%)**
SiO_2	19.42	50.17	51.24	89.21
Al_2O_3	4.86	43.69	41.86	0.55
Fe_2O_3	3.89	2.96	3.23	2.80
CaO	63.75	0.18	0.14	1.04
MgO	1.12	0.37	0.33	4.44
K_2O	0.65	0.81	1.15	0.86
Na_2O	0.13	0.24	0.03	0.14
SO_3	2.99	0.03	0.04	0.23

* Plus other trace elements

3.2.1 Cement

The cement used was an ASTM C 150 Type I/II provided by a local cement producer. The decision to use a Type I/II was based on increasing the workability of the mix versus the use of a fast strength gaining Type III cement. The loss of early age strength was not seen as issue due to the overall mix designs and the benefits of the SCMs used, such as silica fume and metakaolin.

3.2.2 Supplementary Cementitious Material

This study looked at two different SCMs, silica fume and metakaolin. Although the goal was to use local materials when possible, both SCMs were obtained from outside the state of Texas. Silica fume was mentioned earlier in this report as a pozzolan. Metakaolin is a natural pozzolan and has the similar benefits to silica fume including pore blocking and converting CH to C-S-H. These materials were chosen because of their impact on compressive strength and the durability of the concrete as discussed in the overview of silica fume in this report.

The silica fume is distinguishable with a dark greyish color and the metakaolin is distinguishable with a tan almost pink color shown in Figure 22 and Figure 23 respectively.

Figure 22: Silica fume color

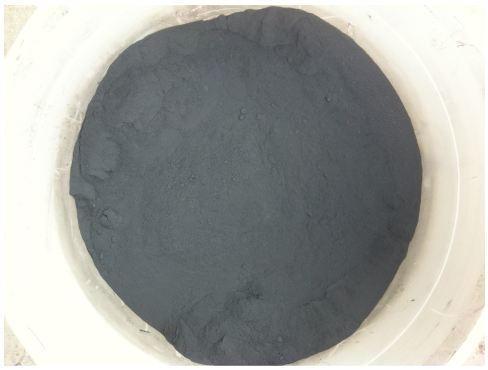

Figure 23: Metakaolin color

3.2.3 Aggregate

The single aggregate used for the nonproprietary mix was a local river sand with a maximum size smaller than a No. 4 sieve. In order to ensure no aggregates larger than 3/8 inch were in the mix, the sand was sieved with a No. 4 sieve. This was done mainly to ensure the high shear mixer would not get damage from a large aggregate getting lodged in a paddle. The sand was kept in an outdoor bin shown in Figure 24. The relevant

properties of this sand are shown in Table 15 and Table 16. Due to the moisture within the aggregates, a moisture correction was applied using ASTM C 566 *Standard Test Method for Total Evaporable Moisture Content of Aggregate by Drying*. The aggregates were batched the day before and mixed for a couple minutes to ensure uniformed moisture. The moisture corrections were applied and the water and aggregate amount was adjusted as needed.

It is worth noting the standard for compressive strength of cubes recommends the use of a graded standard sand. The decision to not use the graded standard sand was to replicate field use of the nonproprietary mix and to take advantage of a locally available river sand.

Figure 24: Outdoor bin for local river sand

Table 15: Local river sand gradation

Sieve No.	**Cum % Retained**
4	0.9
8	11.8
16	28.2
30	54.3
50	86.1
100	97.8

Table 16: Local river sand specifications

Fineness Modulus	2.79
Bulk Specific Gravity (Oven Dry)	2.59
Absorption Capacity (%)	0.56

3.2.4 Fiber

The polyvinyl alcohol (PVA) fibers and steel used in the non-proprietary mixes are shown in Figure 25 and Figure 26. The steel fibers were commercially available and were selected because the same fibers were used in the proprietary mix. The PVA fibers were chosen for comparison and because they are the primary fibers used for ECC developed by Li (Li, 2007). The specifications of the fibers can be seen in Table 17.

Figure 25: PVA fibers close up

Figure 26: Steel fibers close up

Table 17: Fiber characteristics

	Steel Fiber	**PVA Fiber**
Length	0.5 in	0.375 in
Diameter	.0079 in	8 denier
Specific Gravity	7.85	1.3
Tensile Strength	313 ksi	210 ksi
Young's Modulus	± 30,450 ksi	-

3.2.5 Admixtures

The admixtures used were a high range water reducer (HRWR) and normal water reducing retarder. The HRWR is a polycarboxylate meeting the ASTM C 494 standard for a Type A and F water reducer and high range water reducer and has a specific gravity of roughly 1.08. The recommended dosage of the HRWR used is up to 12 fl.oz. / 100 lbs although per the manufacturer, this dosage could be exceeded for materials using microsilica without any issues.

The normal water reducer meets the ASTM C 494 standard for a Type B and D water reducing and retarding admixtures and has a specific gravity of roughly 1.18. The recommended dosage of the normal water reducer is 2-4 fl.oz. / 100 lbs. For this project, the dosage for the Type B and D was never taken past the recommended limits.

The combined use of both water reducers is a common practice in central Texas to help save costs from the HRWR while still achieving the workability required. During mixing, the water is split into two different containers with the normal water reducer in one container and the HRWR in the other. The normal water reducer was placed first and acts as a good lubricant for the aggregates. The mixing procedure will be discussed in greater detail in the following section.

3.3 MIXING, CASTING AND CURING OF UHPC

The mixing and casting and curing of UHPC followed ASTM C 192 *Standard Practice for Making and Curing Concrete Test Specimens in the Laboratory* with some variations discussed later. A 3 ft^3 vertical shaft mixer shown in Figure 27 was used to mix the materials. The basic specifications of the mixer are shown in Table 18. In addition, the mixer is able to rotate the paddles in reverse to ensure thorough mixing of the material. The use of a vertical shaft mixer was decided as recommended by the proprietary mix manufacturer.

Figure 27: Vertical shaft mixer used for UHPC

Table 18: Vertical shaft mixer specifications

Batch Output	3 cu. ft.
Motor Rating	2 hp/ 15 amps/ 110V
Paddle Speed	38 RPM
Max Aggregate Size	3/8”

The mixing of the proprietary mix followed the same procedure from the FHWA report by Graybeal shown below (Graybeal, 2006). Each mix came in premixed 50-lb bags that were opened directly into the high shear mixer as shown in Figure 28.

1. Weigh all materials and add half HRWA to water
2. Place premix bags in pan and mix for 2 minutes
3. Add water (with half HRWA) to premix over 2 minutes
4. Wait 1 minute, then add remaining HRWA over 30 seconds
5. Wait 1 minute, then add accelerator over 1 minute
6. Continue mixing until the mix turns from a dry powder to a thick paste (time may vary)
7. Add fibers to mix over 2 minutes
8. Mix for an additional 1 minute to ensure dispersion of fibers

Figure 28: 50 lb. proprietary mix bags

The process for mixing the nonproprietary mix was similar with minor variations shown below.

1. Weigh all materials adding HRWR to half the water and water reducing retarder (if used) to other half of water
2. Add sand and water with water reducing retarder (if used) to mixer and mix for 1 minute
3. Stop mixer and add cement and supplementary cementitious material to pan and mix for 30 seconds
4. Add water with half HRWR over one minute
5. Mix materials until the UHPC is observed to self-level (reverse paddles if necessary to ensure mixing of the material). Time may vary
6. Add fibers to mix over 1 minute
7. Mix for an additional 1 minute to ensure dispersion of fibers

Each mix was mixed and samples cast in an environmentally controlled room set at 73 ± 3 °F. As soon as mixing was complete, the casting of the specimens and measuring

of the flow started. As discussed later in this report, the flow was tested using a modified version of ASTM C 1437.

The specimens were casted as soon as possible to avoid initial set of the mix. The filling of the molds was accomplished with the use of scoops. The three by six cylinders were casted in two layers with each layer rodded 25 times. Due to the fiber orientation not being of much importance compared to beams, the rodding of the fibers was determined to not be a significant issue. The cube molds were casted using scoops and filled following ASTM C 109. Each cube was casted in two layers with each layer tamped with a rubber tamper 32 times in four rounds. The beams were casted with a scoop with special attention on the orientation of the fibers. In order to allow the fibers to flow along the length of the beam, no vibration was applied. In addition, the material was placed on one end and allowed to flow to the other end. If the material did not flow as desired, the beam mold was lifted on one end and tamped on the sides. After all the specimens were filled, they were all screeded using a wooden trowel. Afterwards, the cylinders were capped with a plastic lid and the beams and cubes were covered with a plastic sheet and wet burlap to prevent moisture loss. The wet burlap was not added until initial set occurred.

Demolding of the specimens occurred 24 hours after the water was added to the cement. Afterwards, each specimen was marked with a unique identifier. The cylinders and beams were placed in an environmental controlled fog room set at 73 ± 3 °F until the time of testing. The cubes were placed in a lime bath immediately after demolding and kept in it until testing inside an environmental controlled room set at room temperature.

3.3.1 Mix Designs

The mix design for the nonproprietary mixes stayed constant between different batches in terms of cement, water and sand amount. The batches varied only in SCM type, SCM amount, fiber type, and fiber amount. These mix designs were selected to optimize the SCM and fibers in the non-proprietary mixes. With the exception of one batch, the amount of SCM was kept constant at 225 lb/yd^3. The difference was due to the practice of using 50% more metakaolin compared to silica fume in central Texas for comparable results. The increased amount of metakaolin for this particular mix was not as workable and as a result, a mix with 225 lb/yd^3 of metakaolin was developed. The water to cement ratio was kept at 0.33. This is a relatively high value when looking at typically UHPC mix with a w/c ratio as low as 0.15. Due to the desired compressive strength from TxDOT of 15 ksi, a lower w/c ratio was not studied although a high compressive strength would be expected.

Table 19: UHPC mix designs

Batch	Cement (lb/yd^3)	Water (lb/yd^3)	Sand (lb/yd^3)	SCM (lb/yd^3)	Fibers by volume
U-SF-S2	1500	500	1600	225	2% Steel Fibers
U-SF-S2*	1500	500	1600	225	2% Steel Fibers
U-SF-S1.5	1500	500	1600	225	1.5% Steel Fibers
U-SF-S1.5*	1500	500	1600	225	1.5% Steel Fibers
U-SF-S1	1500	500	1600	225	1% Steel Fibers
U-SF-P2	1500	500	1600	225	2% PVA Fibers
U-SF-P1	1500	500	1600	225	1% PVA Fibers
U-MK2-S1	1500	500	1600	450	1% Steel Fibers
U-MK-S2	1500	500	1600	225	2% Steel Fibers
U-MK-S1	1500	500	1600	225	1% Steel Fibers
U-SF-0	1500	500	1600	225	0% Steel Fibers
U-SF-0*	1500	500	1600	225	0% Steel Fibers
UD-S2	-	-	-	-	2% Steel Fibers

3.4 FLOW TESTING

An important characteristic of UHPC is its self-leveling behavior. This allows the material to form itself in small openings such as PBE connections. In order to test this, a modified ASTM C 1497 *Flow of Hydraulic Cement Mortar* was performed using a flow table shown in Figure 29. Instead of presenting the flow in terms of a percentage as described in the standard, the actual diameter of the material was measured pre-tamping (static flow) and post tamping (dynamic flow) in inches shown in Table 20. The diameter of the material was taken (after the material was allowed to reach a steady) at four equally spaced locations and the average was taken. Per the FHWA report, a flow greater than eight

inches is considered adequate for self-leveling properties. During mixing, the workability of a mix was also observed visually. If the mix was able to settle and self-level inside the high shear mixer shown in Figure 30, no further admixtures were added. This visual observation is representative of field conditions when placing UHPC in the PBE connections and allowing the mix to level on its own.

Figure 29: ASTM C 1497 flow table

Figure 30: UHPC mix showing self-leveling behavior

In general, the static flow ranged between four and five and a half inches. The exception to this were the mixes with no fibers and the proprietary mix, which had a static flow of six and seven and three quarters respectively. The effect of fibers was evident in this study. The higher fiber content mixes resulted in a lower flow value. The highest static flow was the proprietary mix which may be due to the optimized aggregate gradation. This behavior of the proprietary mix indicates the minimum amount of consolidating and vibration needed.

The average dynamic flow was taken after applying 25 blows to the material in 15 seconds. The mixes with PVA did not achieve a flow greater than eight inches and also required a considerable amount more admixture compared to the other mixes. This may be due to the interaction of the PVA with the fine silica fume particles. Typical mixes that use PVA fibers such as engineering cementitious composites (ECC) developed by Li uses fly ash instead of silica fume with no issues (Li, 2007). As mentioned earlier, the metakaolin mixes were initially developed using a 22.5% amount versus the 15% used for silica fume. After this mix was found to be less workable, the amount of metakaolin was decreased to 15%. The new metakaolin mixes with 2% and 1% fibers were found to have an acceptable flow.

Some mixes resulted in an average flow greater than 10 inches which indicates a mix that fell off the flow table. For these mixes, further study can be done to optimize the amount of water and admixture used.

Table 20: Flow testing of UHPC

Batch	HRWR (oz/cwt)	Water reducer retarder (oz/cwt)	Average static flow (in)	Average dynamic flow (in.)	Adequate for self-leveling? (>8 in)
U-SF-S2	10	0	4-1/2	8-7/8	Yes
U-SF-S2*	10	2	4-1/2	9	Yes
U-SF-S1.5	10	0	5	9-1/4	Yes
U-SF-S1.5*	10	2	5-1/2	>10	Yes
U-SF-S1	10	0	4-5/8	9-15/16	Yes
U-SF-P2	18†	2	4-3/16	6-7/16	No
U-SF-P1	10	0	4.5	7-1/4	No
U-MK-S1	16	3	4	7-1/4	No
U-MK-S2	12‡	0	4-9/16	8-9/16	Yes
U-MK-S1	12‡	2	5-1/16	>10	Yes
U-MK-0	12‡	2	5-5/16	>10	Yes
U-SF-0	10	0	4-7/8	9	Yes
U-SF-0*	10	2	6	>10	Yes
UD-S2	-	-	7-3/4	8-13/16	Yes

† The amount of HRWR and water reducing retarder was increased after mixing the materials from 10 oz./cwt and 0 oz./cwt respectively to increase workability

‡ The amount of HRWR was increased after mixing materials from 10 oz./cwt to increase workability

3.5 Compression Strength Testing

The compressive strength tests were done using a Forney FX700F-Pilot compression machine following ASTM C 109. The load rate was kept at the upper end of the allowable tolerance around 400 lbs./sec using a manual flow valve. A grinding tool was used to clean the edges of the cubes to ensure planeness of the specimen. An upper

spherical block built just for 2 in cubes was used to ensure conformity with the standard shown in Figure 31.

Figure 31: Compression setup for cubes

Keeping the load rate constant proved to be a challenge and the operator manually adjusted the load rate throughout the test until failure of the specimen. During the initial stages of the study, the compressive strengths of the specimens had standard deviations outside the tolerable limits. The issue was in a safety mechanism of the compression machine that stops the load when the load drops a certain amount. The acceptable load drop was increased in the settings and the specimens were able to have more precise values. Unlike conventional concrete, the failure of UHPC and these fibers in particular was uneventful, without a significant visible failure. None of the mixes experienced a brittle or explosive failure even at the higher strengths. A comparison of a failed specimen with and without fibers is shown in Figure 32 and Figure 33. The specimens with no fibers failed noticeably whereas the specimen with fibers is almost

indistinguishable with a specimen pre-failure. In general, the load rate was easier to control in the middle part of the test but difficult in the beginning and end.

Figure 32: Failed specimen with no fibers

Figure 33: Failed specimen with fibers

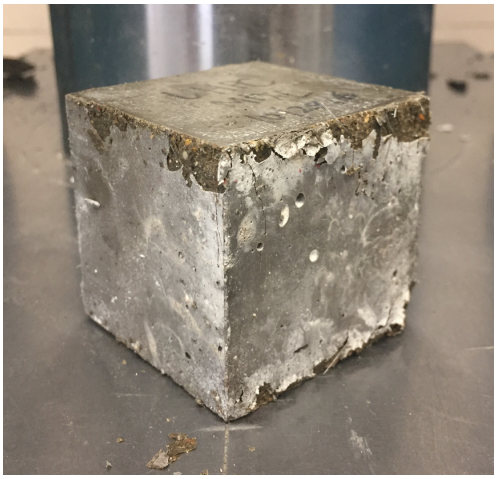

A total of three cubes per age for each mix was tested. The data for the compressive strength values can be seen in Table 21. Figure 34 to Figure 36 shows the compressive strength tests at 1, 7, and 28 curing days respectively. A threshold bar was added at 14 ksi to show when or if the material surpasses the minimum requirement for prefabricated bridge element UHPC connections. Due to the nature of the nonproprietary mix, the specimens did not gain sufficient strength at 24 hours and were instead tested after three days. Outside of the proprietary mix, the largest strength gain after 24 hours was mix U-SF-S1. By seven days, all of the metakaolin mixes and U-SF-S1 reached the 14 ksi threshold. At 28 days, the strength gain for all the mixes slowed down but the threshold was met.

Table 21: Compressive strength data

Batch		**1-Day Compressive Strength**	**7-Day Compressive Strength**	**28-Day Compressive Strength**
U-SF-S2	Maximum load (lbf)	35567	52955	65083
	Compressive strength (psi)	8890	13240	16270
	Standard Deviation	352	1195	2649
	Coefficient of Variation	1%	2%	4%
U-SF-S2*	Maximum load (lbf)	29143	53267	60850
	Compressive strength (psi)	7290	13320	15210
	Standard Deviation	689	510	580
	Coefficient of Variation	2%	1%	1%
U-SF-S1.5	Maximum load (lbf)	34813	54587	64650
	Compressive strength (psi)	8700	13650	16160
	Standard Deviation	482	1227	2153
	Coefficient of Variation	1%	2%	3%
U-SF-S1.5*	Maximum load (lbf)	29553	51652	62450
	Compressive strength (psi)	7390	12910	15610
	Standard Deviation	925	1414	368
	Coefficient of Variation	3%	3%	1%

Table 21: Compressive strength data

Batch		**1-Day Compressive Strength**	**7-Day Compressive Strength**	**28-Day Compressive Strength**
U-SF-S1	Maximum load (lbf)	36060	56980	66067
	Compressive strength (psi)	9020	14250	16520
	Standard Deviation	1061	1092	899
	Coefficient of Variation	3%	2%	1%
U-SF-P2	Maximum load (lbf)	24790	46490	59410
	Compressive strength (psi)	6200	11620	14850
	Standard Deviation	671	2008	2390
	Coefficient of Variation	3%	4%	4%
U-SF-P1	Maximum load (lbf)	28937	42883	60193
	Compressive strength (psi)	7230	10720	15050
	Standard Deviation	1031	1288	2557
	Coefficient of Variation	4%	3%	4%
U-MK2-S1	Maximum load (lbf)	34783	63687	68447
	Compressive strength (psi)	8700	15920	17110
	Standard Deviation	645	751	2171
	Coefficient of Variation	2%	1%	3%

Table 21: Compressive strength data

Batch		**1-Day Compressive Strength**	**7-Day Compressive Strength**	**28-Day Compressive Strength**
U-MK-S2	Maximum load (lbf)	34503	67037	71250
	Compressive strength (psi)	8630	16760	17810
	Standard Deviation	628	870	1270
	Coefficient of Variation	2%	1%	2%
U-MK-S1	Maximum load (lbf)	32997	63777	63943
	Compressive strength (psi)	8250	15940	15990
	Standard Deviation	1011	1036	2534
	Coefficient of Variation	3%	2%	4%
U-SF-0	Maximum load (lbf)	23777	48837	57635
	Compressive strength (psi)	5940	12210	14410
	Standard Deviation	1110	1161	1619
	Coefficient of Variation	5%	2%	3%
U-SF-0*	Maximum load (lbf)	26817	50470	54367
	Compressive strength (psi)	6700	12620	13590
	Standard Deviation	498	1012	1082
	Coefficient of Variation	2%	2%	2%

Table 21: Compressive strength data

Batch		**1-Day Compressive Strength**	**7-Day Compressive Strength**	**28-Day Compressive Strength**
UD-S2	Maximum load (lbf)	53282	70585	98517
	Compressive strength (psi)	13320	17650	24630
	Standard Deviation	613	3019	2194
	Coefficient of Variation	1%	4%	2%

Figure 34: Compressive Strength of UHPC Mixes at 1 Day

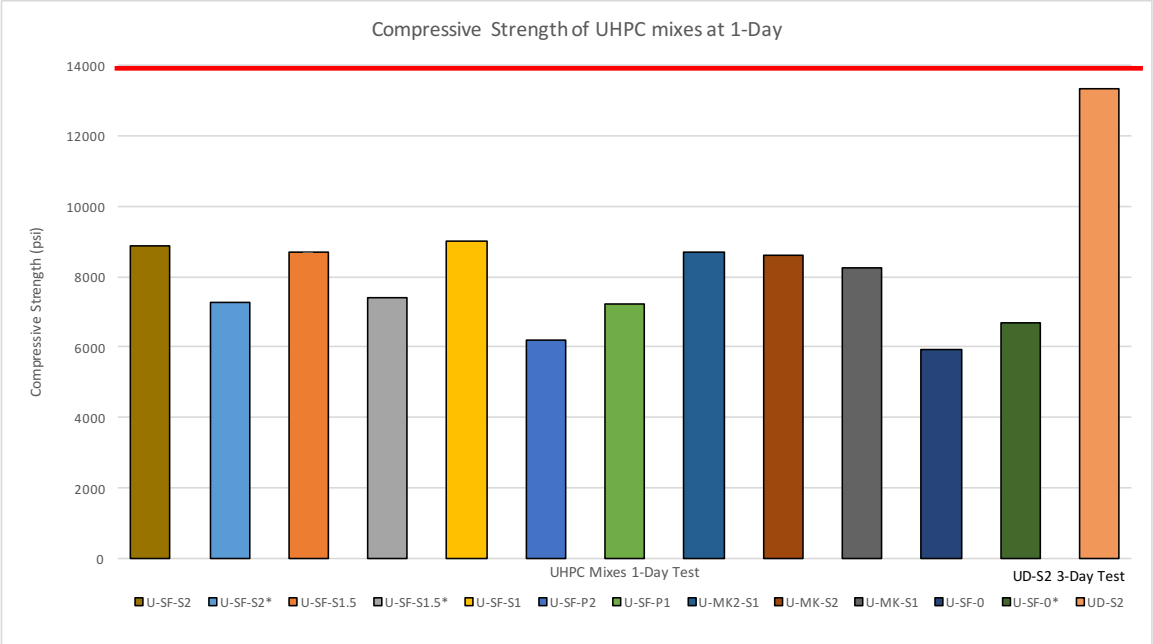

Figure 35: Compressive Strength of UHPC Mixes at 7 Days

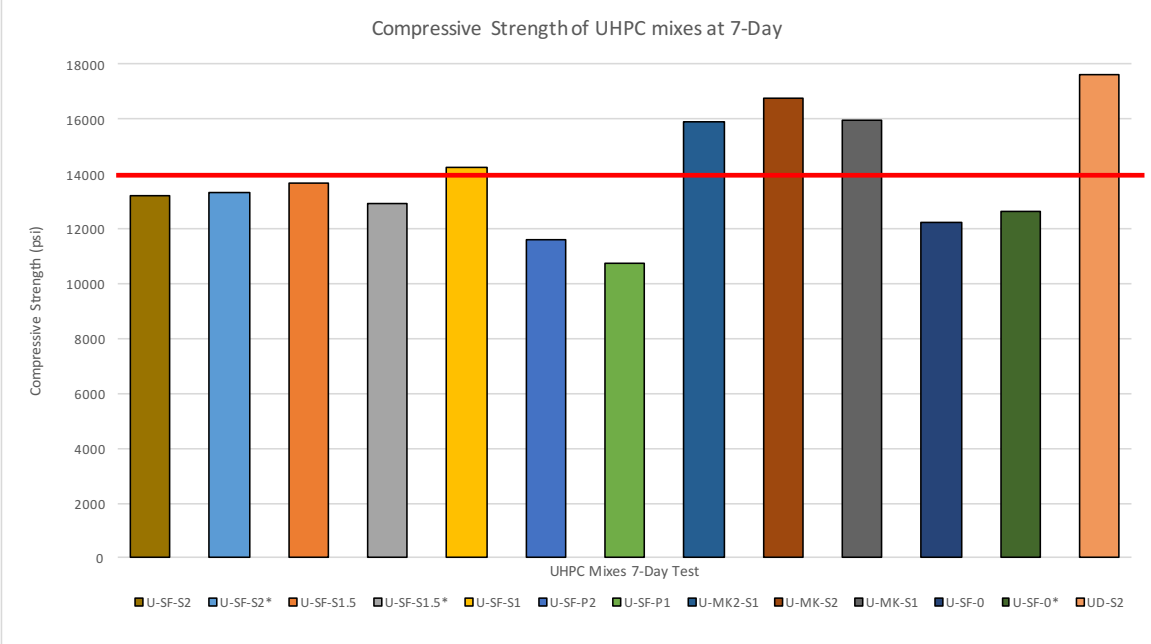

Figure 36: Compressive Strength of UHPC Mixes at 28 Days

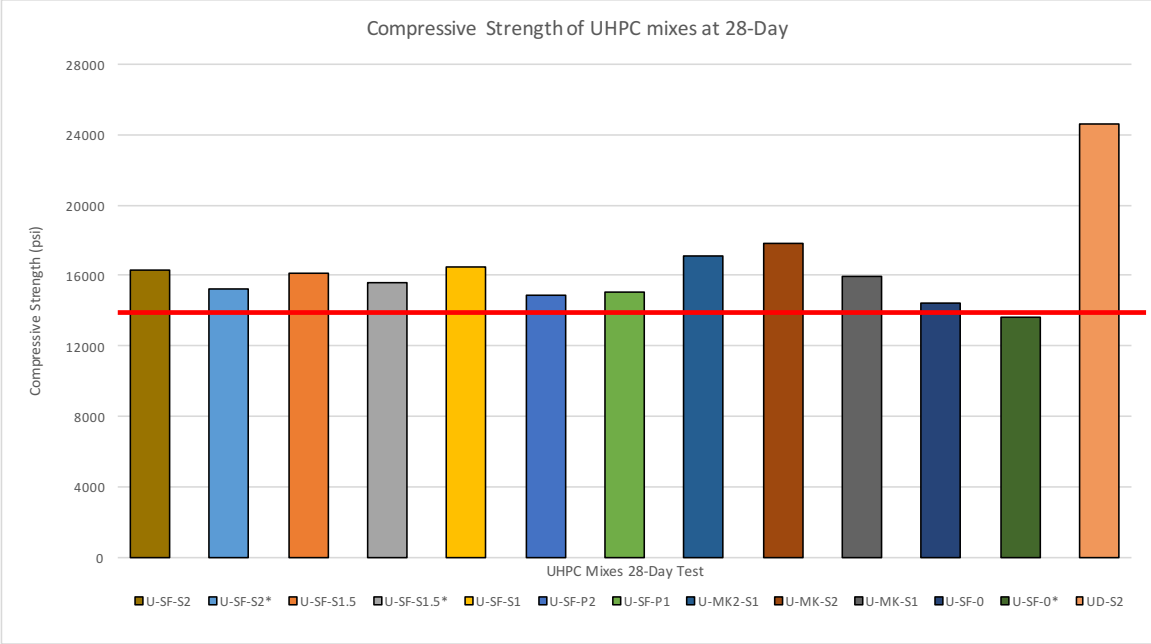

3.5.1 Effect of Steel Fibers on Compressive Strength

The strength gain of UHPC with steel fibers and 15% silica fume is shown in Figure 37. The benefits of silica fume are shown immediately with a majority of the strength gain after 24 hours and tapering off afterwards with little strength gain from 7 to 28 days. Also shown is the impact of steel fibers on the compressive strength. The increase from the mix without fibers to the mix with 2% fibers shows an increase of roughly 50%. This increase follows nicely the expected impact of fibers on compressive strength shown in Table 8 from an earlier section. Interestingly, increasing the amount of fibers decreased the compressive strength at least for these mixes. This may be due to difficulty of packing and consolidation with higher fiber amounts.

Figure 37: Compressive Strength of UHPC with 0,1,1.5 and 2% Steel Fibers and 15% Silica Fume

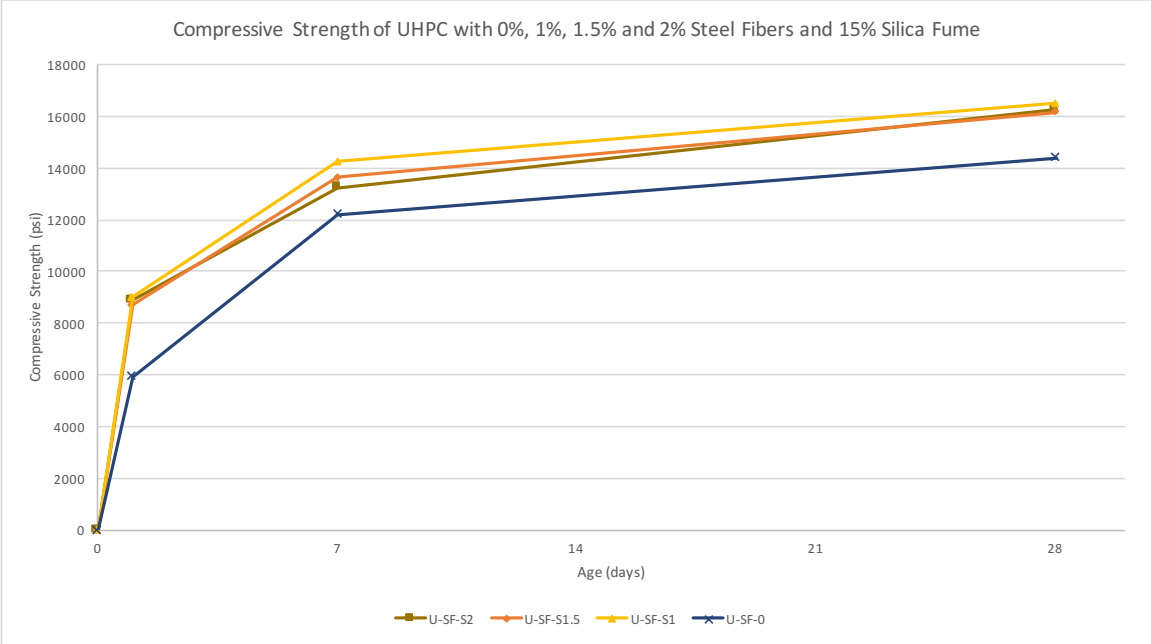

3.5.2 Effect of PVA Fibers on Compressive Strength

The strength gain of PVA mixes over time are shown in Figure 38. Due to the increased number of admixtures in these mixes, the early age strengths were comparably lower to the other mixes. The impact of the increased admixtures in U-SF-P2 is shown in the one day age with the strengths being more than 1,000 psi less than U-SF-P1. Unlike the steel fibers, packing of PVA is not seen as much of an issue because of its ability to bend versus the steel fibers. As such, the compressive strength shows no noticeable correlation between the amount of PVA fibers and compressive strength. In addition, a comparison with U-SF-0 does not show as large a contribution of fibers to the compressive strength as much as the steel fiber mixes.

Figure 38: Compressive Strength of UHPC with 1 and 2% PVA with 15% Silica Fume

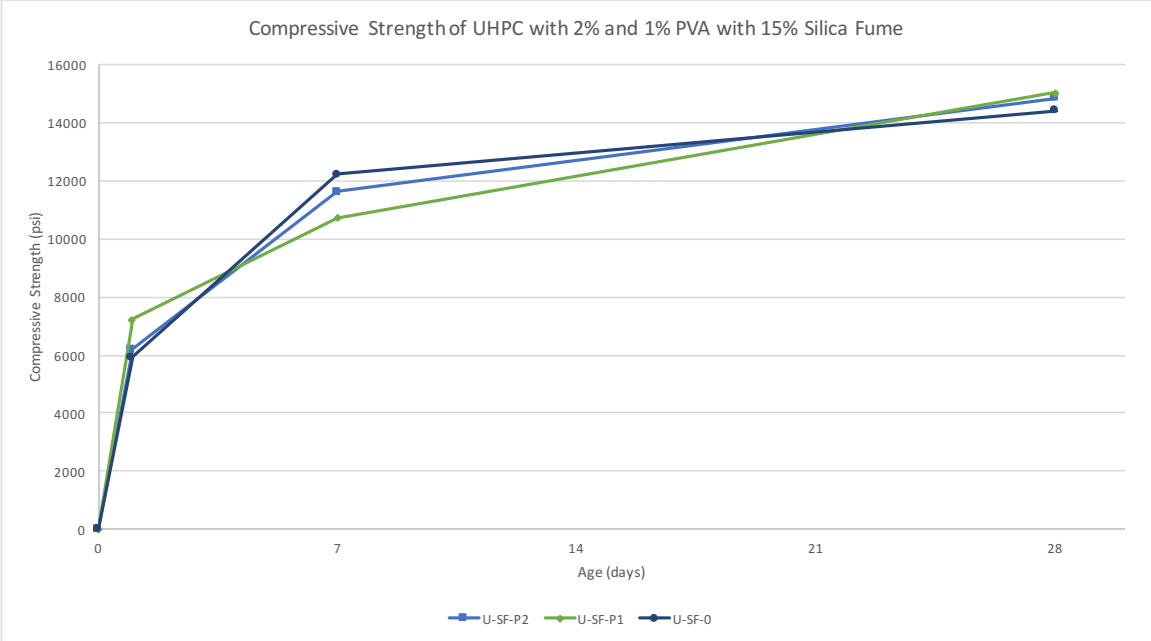

3.5.3 Effect of Metakaolin on Compressive Strength

The compressive strength gain with the metakaolin mixes are shown in Figure 39. In comparison, the seven day mixes with metakaolin show a tremendous strength gain at seven days compared to the mixes with silica fume. However, this effect is quickly tempered and the strengths show little to no increase between 7 in 28 days. It is worth pointing out that the metakaolin mixes show an increase in compressive strength with the presence of more fibers. Also, there was a discernible difference between U-MK2-S1 U-MK-S1, with the former showing higher strengths. As a reminder, the 15% mix was developed due to the workability issues with mix U-MK2-S1. Mix U-MK2-S1 was tested at six days as opposed to seven although the trajectory would have shown more of an increase at seven days compared to U-MK-S1.

Figure 39: Compressive Strength of UHPC with 1 and 2% Steel Fibers with 15% and 22.5% Metakaolin

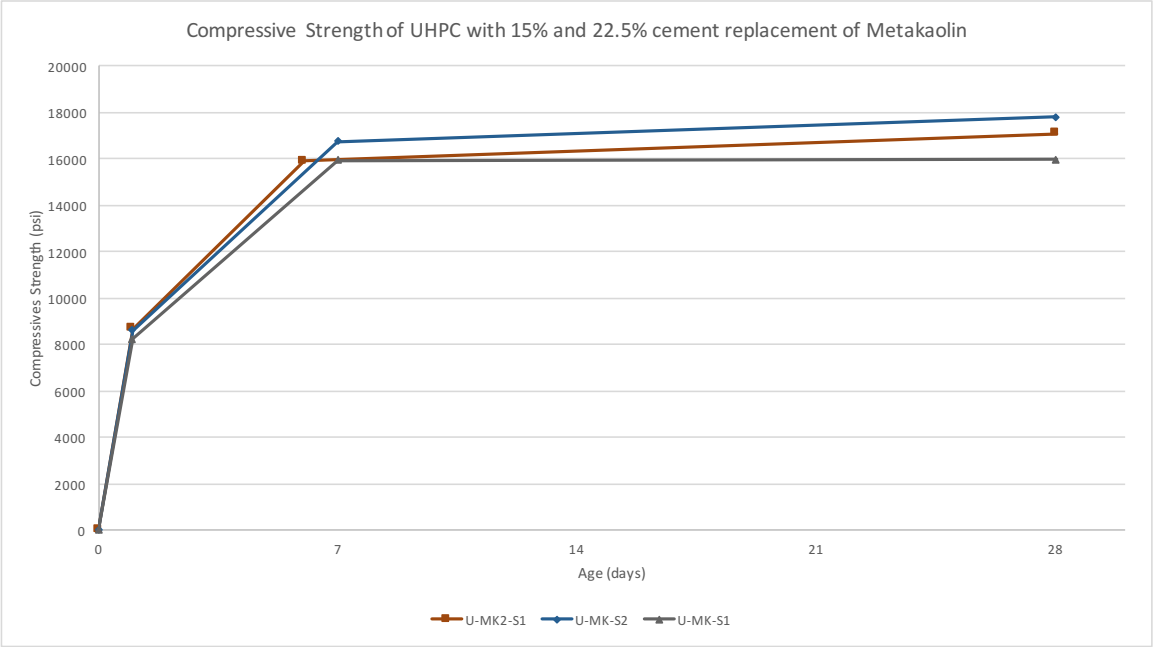

3.5.4 Effect of Load Rate on Compressive Strength

A small study on the effect of load rate on compressive strength was done. Increasing the load rate allows the test to take less time due to the high strength values of UHPC. Typically, an increased load rate leads to high compressive strengths. Three mixes at the load rate from the standard of 200 to 400 lbs/sec was compared with three mixes at 600 lbs/sec (150 psi/sec) at 1,7 and 28 days. Mix U-SF-S2* was compared with cubes casted in the same batch at the increased load rate.

The results from the study are shown in Table 22. The higher load rate was found to be difficult to control and thus resulted in a larger variation in the early age. The seven-day age specimens have a higher strength and naturally gave more time for the load rate to settle. The standard deviation and coefficient of variation were calculated treating both load rates as a single batch. The values obtained were acceptable with the seven ages having better results compared to the one day and 28-day age. Based on this study, it appears increasing the load rate to 150 psi/secs has little impact on the compressive strength of the cube. However, there may be some variation in results.

Table 22: Effect of load rate on compressive strength

Load Rate	**Average 1-Day (psi)**	**Average 7-Day (psi)**	**Average 28-Day (psi)**
100 psi/secs	7290	13320	15210
150 psi/secs	6840	13600	16110
Standard Deviation	1876	788	2405
Coefficient of Variation	6.6%	1.5%	4%

3.5.5 Effect of Specimen Geometry on Compressive Strength

Another study was performed looking at the impact of specimen geometry on the compressive strength mainly comparing 3 in x 6 in cylinders with 2 in x 2 in x 2 in cubes. The results are shown in Table 23. The one day strengths show the cylinders trailing the cube strengths nicely. However, the later age strengths show differences in strength of up to 28.5%. The reason in the variation is mostly due to the capping of the cylinders. As discussed earlier, it is recommended the ends of the cylinders are grinded to meet planeness requirements with sulfur capping only used for early age testing. However, without an end grinder, sulfur capping was the only available method to ensure planeness. It should be noted the sulfur compound used was rated for 8788 psi by the manufacturer which may have played a factor in the variation for later age strengths (Appendix A).

Table 23: Effect of specimen geometry on compressive strength

Batch	**Average 1-Day (psi)**	**Average 7-Day (psi)**	**Average 28-Day (psi)**
Cubes (2 in x 2 in x 2 in)	7290	13320	15210
Cylinders (3 in x 6 in)	7220	10000	12000
% Difference	0.98	28.5	23.6

3.5.6 Effect of Admixtures on Early Age Strength

The use of the normal water reducer increases the workability of the mix but at the cost of the early age strength. Table 24 shows the one day and seven day compressive strengths of four mixes, two of which had 2 oz./cwt of the water reducing retarder added. The early age strength strengths show a significant decrease in compressive strength of up to almost 20%. However, the strength from the increased admixture catches up by seven days. Based on this study, it is unlikely that the increased admixture has any long-term effect on the mixes.

Table 24: Effect of water reducing retarder on early age strength

Batch	**1-Day Compressive Strength (psi)**	**7-Day Compressive Strength (psi)**
U-SF-S2	8890	13240
U-SF-S2*	7290	13320
% difference	19.9%	0.6%
U-SF-S1.5	8700	13650
U-SF-S1.5*	7390	12910
% difference	16.3%	5.5%

3.6 TENSILE STRENGTH TESTING

The splitting tensile tests were performed using a Forney F250EX compression machine shown in Figure 40. The testing set up followed ASTM C 496 to ensure the cylinder was centered in the machine shown in Figure 41. After placement, the cylinders were loaded at a constant rate within 100 to 300 psi/min using a manual pressure valve. At this load rate, a single specimen can take close to 20 minutes before failure. Due to the presence of fibers, there were some challenges with the specimens. One of those challenges was determining when the first crack occurred. In general, the crack was noticeable via an audible crack accompanied with a drop in load rate. However, there were some instances when determining the first crack proved difficult most noticeably for the specimens with 1.5% and 2% steel fibers. For these fibers, the first crack was determined visually although not as accurately. The ultimate strength does not fail in a brittle manner and is determined to be when the material is no longer able to take any load. Figure 42 shows a good example of a failed specimen with the fibers engaged and pulled out verses fracturing.

Figure 40: Forney F250EX machine used for splitting tensile strength tests

Figure 41: Splitting tensile strength setup

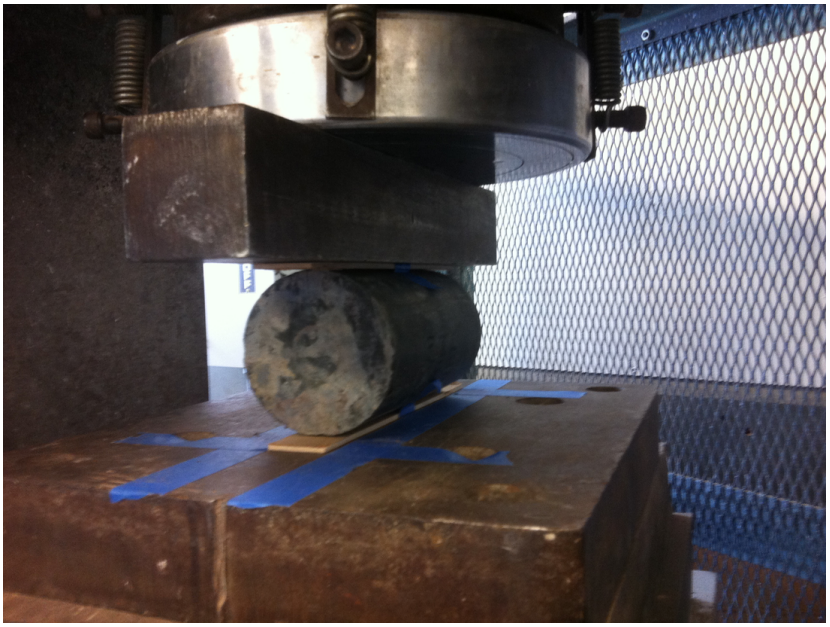

Figure 42: Failed splitting tensile specimen

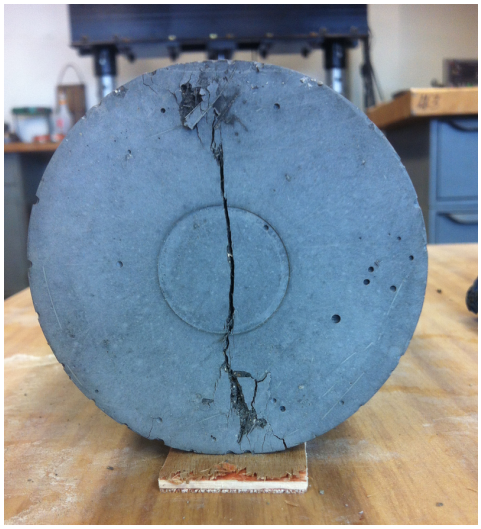

The values from the splitting tensile strength test are shown in Table 25. A total of three specimens per age of every mix was tested to obtain the averages. The one-day cracking strength of U-SF-S2 is an example of not having an audible crack with a coefficient of variation of 12%. Although the test may not be the most accurate for fibers, it still provides some nice data for comparison. For all the ages, the ultimate tensile strength increased as the fiber amount increased, as shown in Figure 43 to Figure 45. The cracking and ultimate tensile strengths showed very little increased between 7 and 28 day strengths. In addition, the highest strengths observed were from the proprietary mix followed by the metakaolin mixes, the silica fume mixes, and the PVA mixes. In order to look at accuracy of the audible method for cracking, a mix without fibers was tested. The mixes without fibers should have similar cracking strengths to the mixes with fibers due to the fibers not being engaged until after first crack. In general, the mixes with fibers had a first crack strength around the same value of the ultimate strength of the mixes without fibers with

the exception of some mixes where it was difficult to determine first crack. Figure 43 to Figure 45 shows a relatively similar bar length across the mixes for the first crack strength. Although not ideal, the audible method provides an adequate means to determine the first crack of a mix with fibers.

Table 25: Splitting tensile strength data

Batch		**1-Day Cracking**	**1-Day Ultimate**	**7-Day Cracking**	**7-Day Ultimate**	**28-Day Cracking**	**28-Day Ultimate**
U-SF-S2	Average Load (lbf)	34833	39771	24500	48082	25825	50111
	Tensile Strength (psi)	1230	1410	870	1700	915	1770
	Standard Deviation	4100	2078	500	2453	2088	2598
	Coefficient of Variation	12%	5%	2%	5%	8%	5%
U-SF-S2*	Average Load (lbf)	21052	34776	23772	42046	26540	53016
	Tensile Strength (psi)	745	1230	840	1490	940	1875
	Standard Deviation	1050	243	496	292	1558	3943
	Coefficient of Variation	5%	1%	2%	1%	6%	7%
U-SF-S1.5	Average Load (lbf)	21950	31855	24170	41799	24824	47088
	Tensile Strength (psi)	775	1125	855	1480	880	1665
	Standard Deviation	2937	645	1267	474	239	706
	Coefficient of Variation	13%	2%	5%	1%	1%	1%

Table 25: Splitting tensile strength data

Batch		1-Day Cracking	1-Day Ultimate	7-Day Cracking	7-Day Ultimate	28-Day Cracking	28-Day Ultimate
U-SF-S1.5*	Average Load (lbf)	20019	30604	24243	41554	28221	47364
	Tensile Strength (psi)	710	1080	860	1470	1000	1675
	Standard Deviation	2014	1282	1244	510	229	2134
	Coefficient of Variation	10%	4%	5%	1%	1%	5%
U-SF-S1	Average Load (lbf)	19333	33054	25301	38447	28994	45299
	Tensile Strength (psi)	685	1170	895	1360	1025	1600
	Standard Deviation	569	1864	2903	3656	1191	2698
	Coefficient of Variation	3%	6%	11%	10%	4%	6%
U-SF-P2	Average Load (lbf)	22862	24674	19969	32583	27256	40609
	Tensile Strength (psi)	810	875	705	1150	965	1435
	Standard Deviation	820	1620	1619	2336	1155	500
	Coefficient of Variation	4%	7%	8%	7%	4%	1%
U-SF-P1	Average Load (lbf)	18094	26684	21594	33381	28172	37761
	Tensile Strength (psi)	640	945	765	1180	995	1335
	Standard Deviation	936	686	724	1124	514	1602
	Coefficient of Variation	5%	3%	3%	3%	2%	4%

Table 25: Splitting tensile strength data

Batch		1-Day Cracking	1-Day Ultimate	7-Day Cracking	7-Day Ultimate	28-Day Cracking	28-Day Ultimate
U-MK2-S1	Average Load (lbf)	17954	33794	21705	44222	28349	50754
	Tensile Strength (psi)	635	1195	770	1565	1005	1795
	Standard Deviation	945	976	2432	3279	1228	1566
	Coefficient of Variation	5%	3%	11%	7%	4%	3%
U-MK-S2	Average Load (lbf)	20511	37297	20737	54660	25794	58875
	Tensile Strength (psi)	725	1320	735	1935	910	2080
	Standard Deviation	399	2164	896	3620	1701	2483
	Coefficient of Variation	2%	6%	4%	7%	7%	4%
U-MK-S1	Average Load (lbf)	20842	33187	26793	45522	25997	53014
	Tensile Strength (psi)	740	1175	950	1610	920	1875
	Standard Deviation	1050	1694	2248	399	1142	967
	Coefficient of Variation	5%	5%	8%	1%	4%	2%
U-SF-0	Average Load (lbf)	-	21180	-	22200	-	25951
	Tensile Strength (psi)	-	750	-	785	-	920
	Standard Deviation	-	476	-	2945	-	2277
	Coefficient of Variation	-	2%	-	13%	-	9%

Table 25: Splitting tensile strength data

Batch		1-Day Cracking	1-Day Ultimate	7-Day Cracking	7-Day Ultimate	28-Day Cracking	28-Day Ultimate
U-SF-0*	Average Load (lbf)	-	15764	-	20875	-	25828
	Tensile Strength (psi)	-	560	-	740	-	915
	Standard Deviation	-	836	-	464	-	1534
	Coefficient of Variation	-	5%	-	2%	-	6%
UD-S2	Average Load (lbf)	27983	44035	34720	62154	47384	86200
	Tensile Strength (psi)	990	1560	1230	2200	1675	3050
	Standard Deviation	1861	2563	2856	1945	4595	1379
	Coefficient of Variation	7%	6%	8%	3%	10%	2%

Figure 43: Splitting Tensile Strength of UHPC Mixes at 1 Day

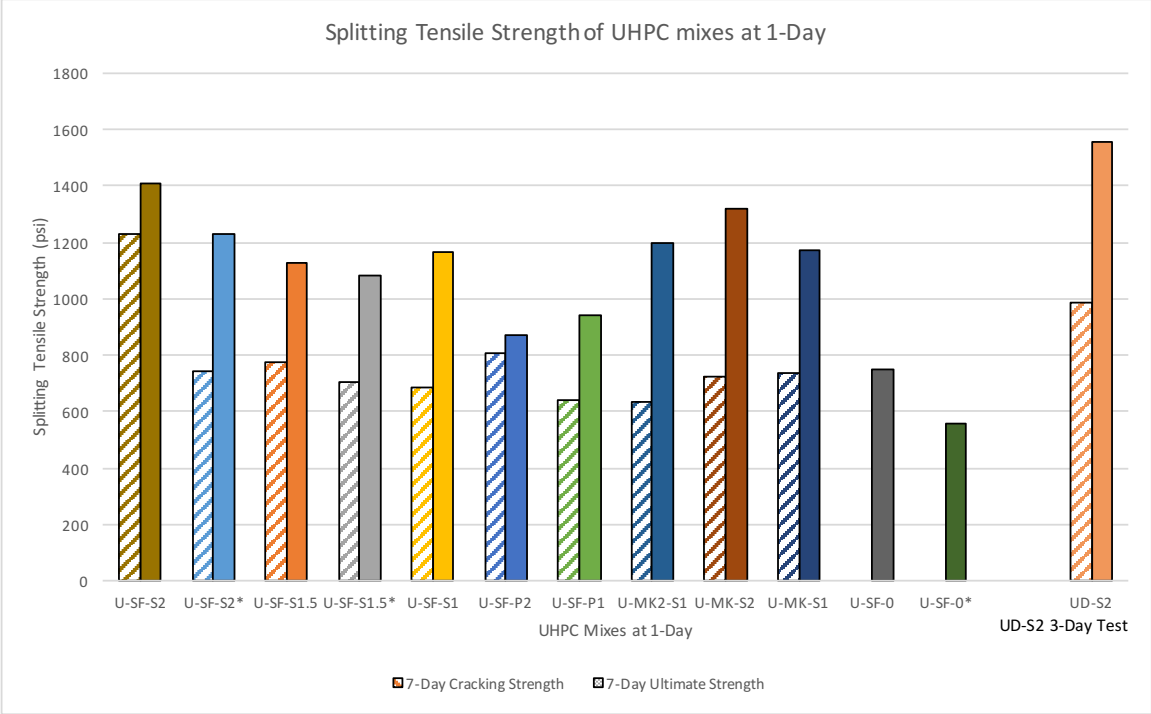

Figure 44: Splitting Tensile Strength of UHPC Mixes at 7 Days

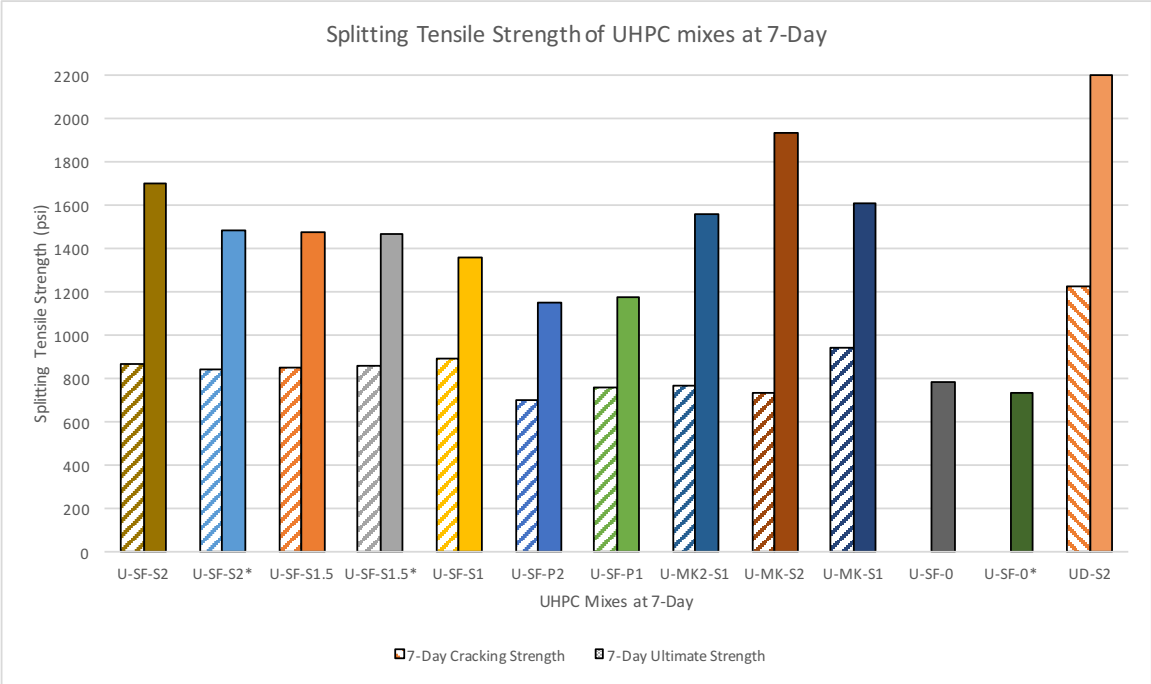

Figure 45: Splitting Tensile Strength of UHPC Mixes at 28 Days

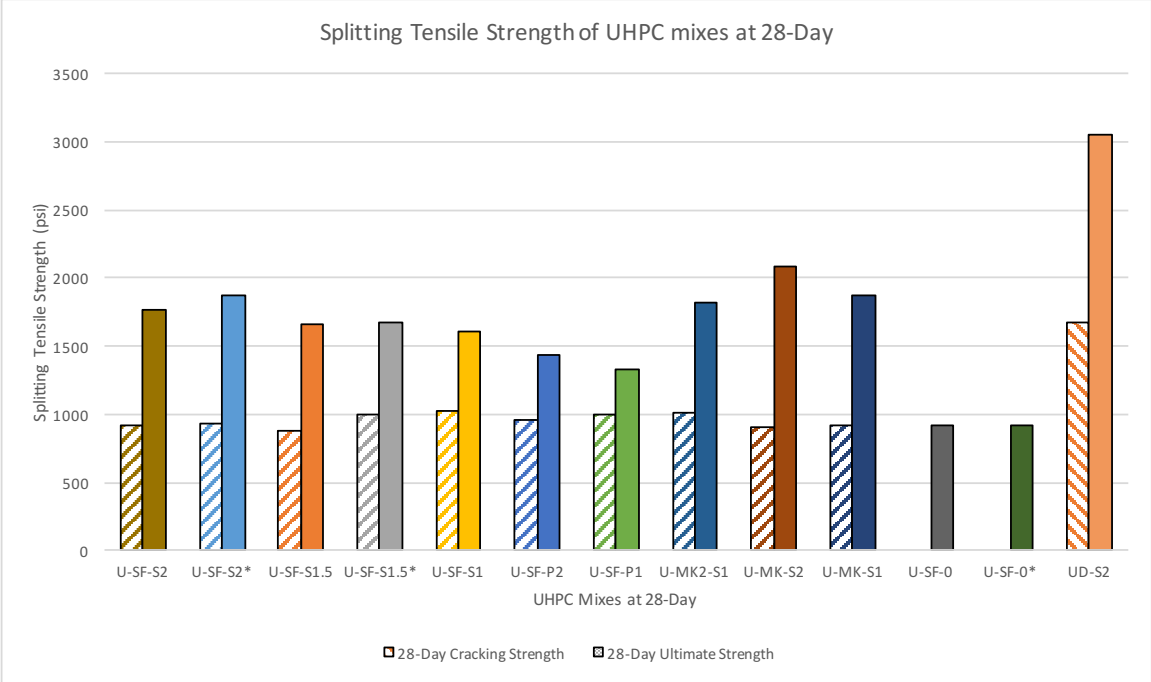

3.7 Modulus of Elasticity Testing

The modulus of elasticity test was performed following ASTM C 469. The machine used to conduct the tests is the same Forney one used for compression testing. Prior to testing, each cylinder was sulfur capped and allowed to cure overnight. During testing day, the cylinders were placed in a compressometer and a level was used to ensure proper fitting (Figure 46). The cylinders were loaded at a constant rate of 35 ± 7 psi/sec using a manual pressure valve. Due to the difference in strengths with cubes, the cylinders were taken to 30% of the cube ultimate compressive strengths. This was determined to not make a difference and still kept the concrete in the elastic zone. A total of two specimens per age of each mix was tested. The readings were taken at a gauge reading of .0004 and when the specimen reached 30% of the cube compressive strength. Afterwards, the chord modulus

of elasticity was computed using the equation provided in the standard. The results from the modulus testing can be seen in Table 26.

Figure 46: Compressometer setup for modulus of elasticity test

As expected, the fibers showed little to no effect on the modulus of the specimens shown in Figure 47 to Figure 49. A visual observation of the graphs shows the bars of the nonproprietary mixes hovering around the same values at the different ages. Also, the majority of the modulus gain occurs in the first day and starts to cap off after seven days with very little gain from 7 to 28 day tests. The modulus testing has the greatest variation of the proprietary mix to the nonproprietary mix. This can be due to a number of factors listed below. A possible solution is better consolidation of the nonproprietary mix through the use of a vibration table.

- Better packing from the optimized aggregates of the proprietary mix
- Higher silica fume content from proprietary mix
- Lower water to cement ratio
- Use of stiffer aggregates compared to local river sand

Table 26: Chord modulus of elasticity data

Batch		1-Day Modulus of Elasticity	7-Day Modulus of Elasticity	28-Day Modulus of Elasticity
U-SF-S2	Chord Modulus of Elasticity (ksi)	3800	4600	4750
	Standard Deviation	20.4	85.3	31.5
	Coefficient of Variation	1%	2%	1%
U-SF-S2*	Chord Modulus of Elasticity (ksi)	3650	4550	4950
	Standard Deviation	40.6	29.9	88.2
	Coefficient of Variation	1%	1%	2%
U-SF-S1.5	Chord Modulus of Elasticity (ksi)	3750	4550	4750
	Standard Deviation	-	169.6	117.8
	Coefficient of Variation	-	4%	2%
U-SF-S1.5*	Chord Modulus of Elasticity (ksi)	3700	4500	4750
	Standard Deviation	38.0	54.2	73.4
	Coefficient of Variation	1%	1%	2%
U-SF-S1	Chord Modulus of Elasticity (ksi)	3800	4450	4950
	Standard Deviation	101.7	170.6	40.1
	Coefficient of Variation	3%	4%	1%

Table 26: Chord modulus of elasticity data

Batch		**1-Day Modulus of Elasticity**	**7-Day Modulus of Elasticity**	**28-Day Modulus of Elasticity**
U-SF-P2	Chord Modulus of Elasticity (ksi)	3150	3850	4350
	Standard Deviation	118.7	163.6	36.2
	Coefficient of Variation	4%	4%	1%
U-SF-P1	Chord Modulus of Elasticity (ksi)	3350	4000	4400
	Standard Deviation	146.8	182.2	133.8
	Coefficient of Variation	4%	5%	3%
U-MK2-S1	Chord Modulus of Elasticity (ksi)	3550	4550	4850
	Standard Deviation	26.5	58.4	115.7
	Coefficient of Variation	1%	1%	2%
U-MK-S2	Chord Modulus of Elasticity (ksi)	3500	4600	5200
	Standard Deviation	146.0	66.3	59.8
	Coefficient of Variation	4%	1%	1%

Table 26: Chord modulus of elasticity data

Batch		**1-Day Modulus of Elasticity**	**7-Day Modulus of Elasticity**	**28-Day Modulus of Elasticity**
U-MK-S1	Chord Modulus of Elasticity (ksi)	3500	5000	5000
	Standard Deviation	58.5	18.1	43.4
	Coefficient of Variation	2%	1%	1%
U-SF-0	Chord Modulus of Elasticity (ksi)	3350	3950	4300
	Standard Deviation	44.8	20.6	133.9
	Coefficient of Variation	1%	1%	3%
U-SF-0*	Chord Modulus of Elasticity (ksi)	3300	4100	4450
	Standard Deviation	58.0	75.7	69.3
	Coefficient of Variation	2%	2%	1.5%
UD-S2	Chord Modulus of Elasticity (ksi)	6500	7550	8600
	Standard Deviation	52.0	95.7	125.1
	Coefficient of Variation	1%	1%	1.5%

Figure 47: Modulus of Elasticity of UHPC Mixes at 1 Day

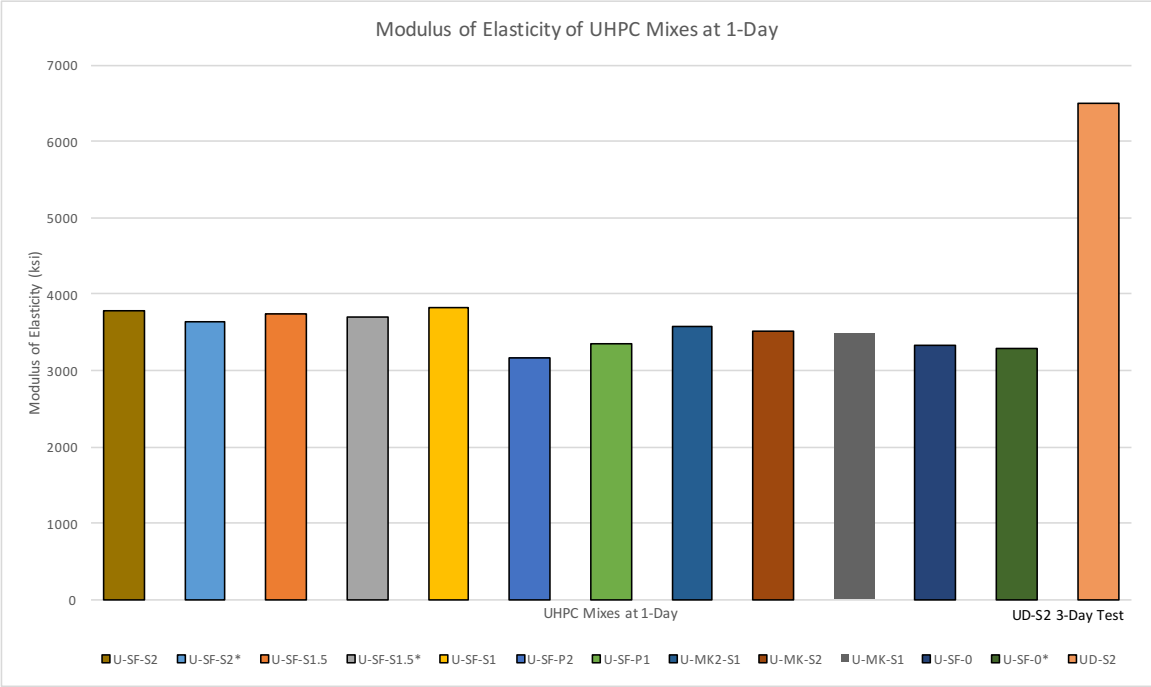

Figure 48: Modulus of Elasticity of UHPC Mixes at 7 Days

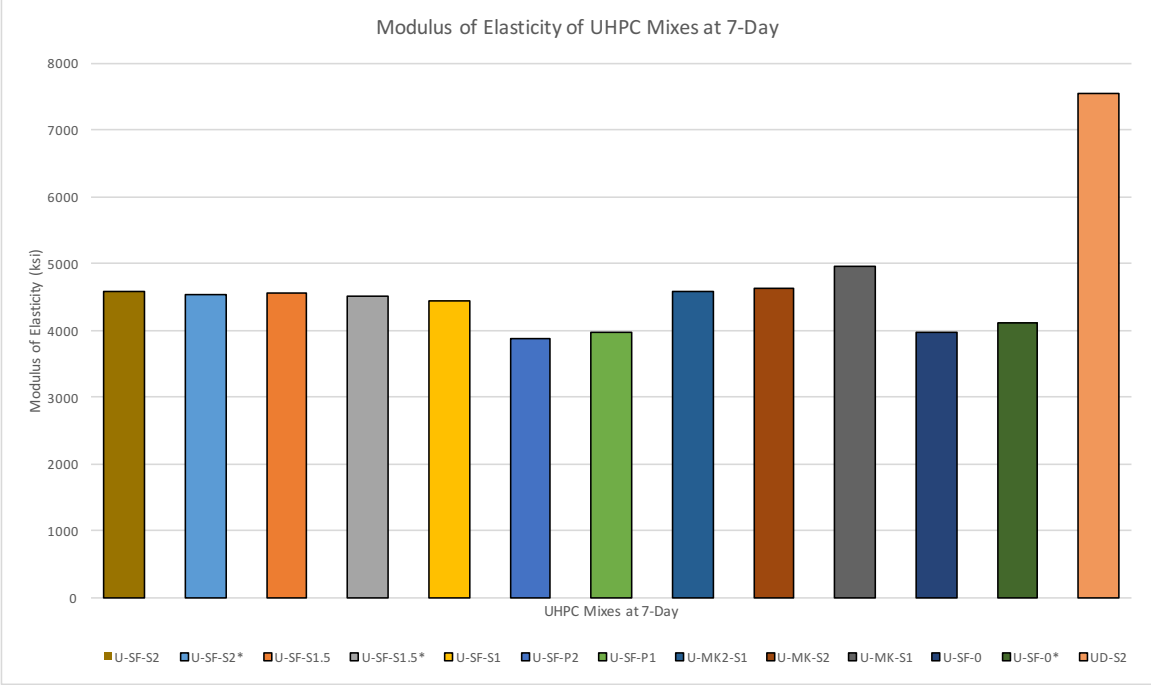

Figure 49: Modulus of Elasticity of UHPC Mixes at 28 Days

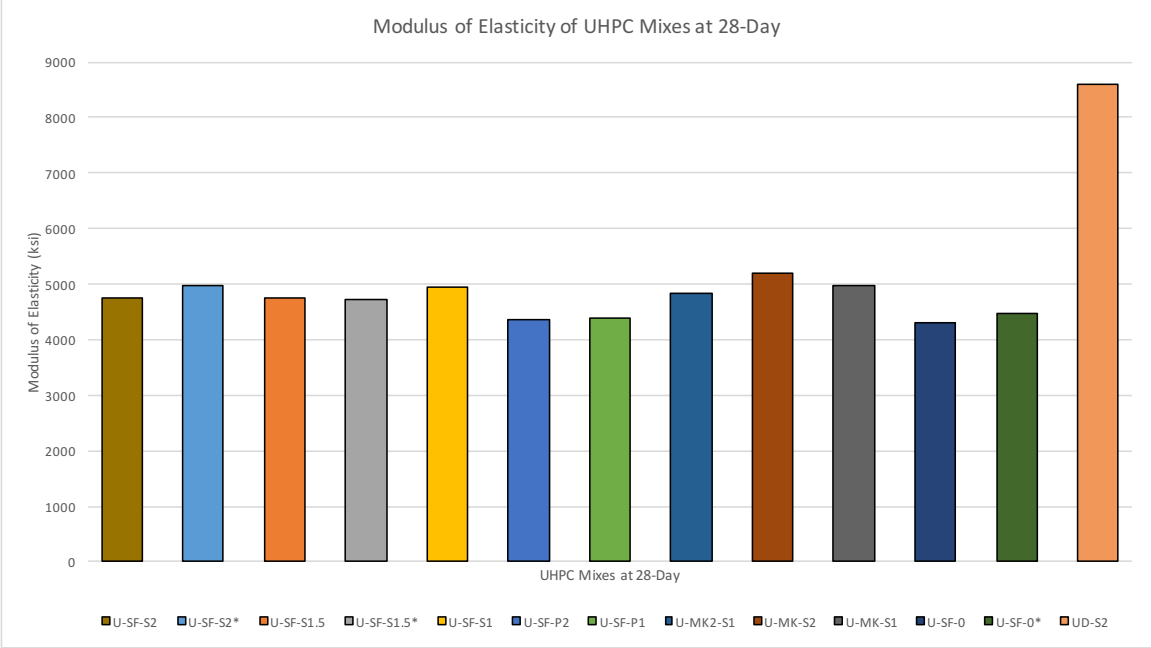

Chapter 4: Conclusions

4.1 Introduction

UHPC is an emerging technology with enhanced mechanical and durability properties. One potential application that has gained a lot of traction in recent years is in prefabricated bridge element connections. The research described in this thesis represents the initial phase of a more comprehensive project aimed at evaluating proprietary and non-proprietary mixes using locally available materials.

4.2 Conclusions

Based on this initial research phase, some conclusions can be drawn, as detailed below:

1. UHPC has significantly improved mechanical and durability properties when compared to conventional concrete
2. Prefabricated bridge element UHPC connections have been proven to be a practical solution in shortening the delivery process and increasing safety in the bridge community
3. UHPC does not fail in a brittle manner and is less explosive than normal concrete
4. The use of steel fibers increases the compressive strength of the material although the greatest improvement is in the toughness of the material allowing the concrete to have a strain hardening behavior post first crack
5. UHPC can have self-leveling properties by using the proper amount of admixture. The development of a nonproprietary mix in Texas is feasible with a majority of the materials being sourced in the state
6. Various non-proprietary mixes were developed that were able to achieve suitable strengths (min. 15 ksi, based on TxDOT feedback) for use in PBE connections

7. The non-proprietary mixes exhibited comparable compressive and tensile strength results to the proprietary mix, but the elastic modulus of the proprietary mix was quite a bit higher than any of the other mixes studied

4.3 FUTURE RESEARCH

This introductory research phase on UHPC will be followed by work related to the following:

1. Evaluation of average residual strength of all UHPC mixes, following ASTM C 1399
2. Further optimization of the nonproprietary mixes, with the intention of improving workability, increasing strength, improving durability, and decreasing cost
3. Long term durability testing of UHPC including exposure sites for ASR and marine environments
4. Field implementation of proprietary and nonproprietary UHPC bridge connections

Appendix A: Sulfur Compound Certificate of Analysis

Georgia Gulf Sulfur Corporation

Since 1959. Dedicated to producing the highest quality sulphur products, manufactured to customer specifications.

Manufacturing Plant: 1300 Spring Creek Road * PO Box 67 * Bainbridge, Georgia 39817 * Ph (229) 246-4552 * Fax (229) 246-3245

Certificate of Analysis

Shipped to: Gilson Company

Lewis Center, OH 43035

Attn: *Chief Chemist*

Date: 7/14/2014
Pickup #: 427
Customer PO#: *BL201957/130193*
Customer Code: *Red Iron 9000*
Quantity: 40000

	Specification	Analysis Test Results		
	Gilson			
	Capping Compound			
	Red Iron 9000	Lot Number	Lot Number	Lot Number
Description:		GN4169001-20		
PURITY	*55-70%*	60.2958%		
ACIDITY				
ASH				
MOISTURE/HEAT LOSS				
OIL				
FINENESS (% through unless noted)				
sive Strength (2 hr cubes)	*7500 Min PSI*	8788		
Cylinder Caps	*Pass-Fail*	Pass		
Viscosity	*2000 CPS Max*	1850		
DATE OF MANUFACTURE		6/19/2014		

This is to advise that the above described shipment meets the specification of the customer code indicated.

GEORGIA GULF SULFUR

Elaine Poitevint
Quality Control Technician

L E Braswell

Chad Braswell
Plant Manager

Form 35
(Certificate of Analysis Program)

References

AASHTO T132 Standard, 2016, "Standard Method of Test for Tensile Strength of Hydraulic Cement Mortars," *AASHTO – American Association of State Highway and Transportation Officials*, Washington, DC, 2016, www.transportation.org.

AASHTO T197 Standard, 2015, "Standard Method of Test for Time of Setting of Concrete Mixtures by Penetration Resistance," *AASHTO – American Association of State Highway and Transportation Officials*, Washington, DC, 2015, www.transportation.org.

AASHTO T259 Standard, 2012, "Standard Method of Test for Resistance of Concrete to Chloride Ion Penetration," *AASHTO – American Association of State Highway and Transportation Officials*, Washington, DC, 2012, www.transportation.org.

AASHTO T260 Standard, 2016, "Standard Method of Test for Sampling and Testing for Chloride Ion in concrete and Concrete Raw Materials," *AASHTO – American Association of State Highway and Transportation Officials*, Washington, DC, 2016, www.transportation.org.

ACI CT-13, 2013. "Concrete Terminology – An ACI Standard," *ACI – American Concrete Institute*, Farmington Hills, MI, 2013, www.aci.org.

ASTM Standard C1018, 1997, "Standard Test Method for Flexural Toughness and First-Crack Strength of Fiber-Reinforced Concrete (Using Beam with Third-Point Loading)." *ASTM International*, West Conshohocken, PA, 1997, www.astm.org.

ASTM Standard C109, 2016, "Standard Test Method for Compressive Strength of Hydraulic Cement Mortars," *ASTM International*, West Conshohocken, PA, 2016, DOI: 10.1520/C0109_C0109M-16A, www.astm.org.

ASTM Standard C1202, 2012, "Standard Test Method for Electrical Indication of Concrete's Ability to Resist Chloride Ion Penetration," *ASTM International*, West Conshohocken, PA, 2012, DOI: 10.1520/C1202-12, www.astm.org.

ASTM Standard C1240, 2015, "Standard Specification for Silica Fume Used in Cementitious Mixtures," *ASTM International*, West Conshohocken, PA, 2015, DOI: 10.1520/C1240-15, www.astm.org.

ASTM Standard C1260, 2014, "Standard Test Method for Potential Alkali Reactivity of Aggregates (Mortar-Bar Method)," *ASTM International*, West Conshohocken, PA, 2014, DOI: 10.1520/C1260-14, www.astm.org.

ASTM Standard C1293, 2015, "Standard Test Method for Determination of Length Change of Concrete Due to Alkali-Silica Reaction," *ASTM International*, West Conshohocken, PA, 2015, DOI: 10.1520/C1293-08BR15, www.astm.org.

ASTM Standard C1399, 2015, "Standard Test Method for Obtaining Average Residual Strength of Fiber-Reinforced Concrete," *ASTM International*, West Conshohocken, PA, 2015, DOI: 10.1520/C1399M-10R15, www.astm.org.

ASTM Standard C1437, 2015, "Standard Test Method for Flow of Hydraulic Cement Mortar," *ASTM International*, West Conshohocken, PA, 2015, DOI: 10.1520/C1437-15, www.astm.org.

ASTM Standard C1497, 2016, "Standard Specification for Cellulosic Fiber Stabilized Thermal Insulation," *ASTM International*, West Conshohocken, PA, 2016, DOI: 10.1520/C1497-16, www.astm.org.

ASTM Standard C1609, 2012, "Standard Test Method for Flexural Performance of Fiber-Reinforced Concrete (Using Beam with Third-Point Loading)," *ASTM International*, West Conshohocken, PA, 2012, DOI: 10.1520/C1609_C1609M-12, www.astm.org.

ASTM Standard C192, 2016, "Standard Practice for Making and Curing Concrete Test Specimens in the Laboratory," *ASTM International*, West Conshohocken, PA, 2016, DOI: 10.1520/C0192_C0192M-16A, www.astm.org.

ASTM Standard C39, 2016, "Standard Test Method for Compressive Strength of Cylindrical Concrete Specimens," *ASTM International*, West Conshohocken, PA, 2016, DOI: 10.1520/C0039_C0039M-16B, www.astm.org.

ASTM Standard C457, 2012, "Standard Test Method for Microscopical Determination of Parameters of the Air-Void System in Hardened Concrete," *ASTM International*, West Conshohocken, PA, 2012, DOI: 10.1520/C0457_C0457M-12, www.astm.org.

ASTM Standard C469, 2014, "Standard Test Method for Static Modulus of Elasticity and Poisson's Ratio of Concrete in Compression," *ASTM International*, West Conshohocken, PA, 2014, DOI: 10.1520/C0469_C0469M-14, www.astm.org.

ASTM Standard C494, 2016, "Standard Specification for Chemical Admixtures for Concrete," *ASTM International*, West Conshohocken, PA, 2016, DOI: 10.1520/C0494_C0494M-16, www.astm.org.

ASTM Standard C496, 2011, "Standard Test Method for Splitting Tensile Strength of Cylindrical Concrete Specimens," *ASTM International*, West Conshohocken, PA, 2011, DOI: 10.1520/C0496_C0496M-11, www.astm.org.

ASTM Standard C566, 2013, "Standard Test Method for Total Evaporable Moisture Content of Aggregate by Drying," *ASTM International*, West Conshohocken, PA, 2013, DOI: 10.1520/C0566-13, www.astm.org.

ASTM Standard C666, 2015, "Standard Test Method for Resistance of Concrete to Rapid Freezing and Thawing," *ASTM International*, West Conshohocken, PA, 2015, DOI: 10.1520/C0666_C0666M-15, www.astm.org.

ASTM Standard C672, 2012, "Standard Test Method for Scaling Resistance of Concrete Surfaces Exposed to Deicing Chemicals," *ASTM International*, West Conshohocken, PA, 2012, DOI: 10.1520/C0672_C0672M-12, www.astm.org.

ASTM Standard C944, 2012, "Standard Test Method for Abrasion Resistance of Concrete or Mortar Surfaces by the Rotating-Cutter Method," *ASTM International*, West Conshohocken, PA, 2012, DOI: 10.1520/C0944_C0944M-12, www.astm.org.

Culmo, Michael, *Accelerated Bridge Construction Experience in Design, Fabrication and Erection of Prefabricated Bridge Elements and Systems Final Manual*. Illinois: Applied Research Associates, Inc., 2011.

Folliard, Kevin. "Portland Cement Hydration." Lecture, University of Texas at Austin, Austin, Texas, 2015.

Graybeal, 2016. "UHPC Connections For ABC." Webinar, ABC-UTC at Florida International University, 2016.

Graybeal, Ben, *Material Property Characterization of Ultra-High Performance* Concrete. Virginia: Turner-Fairbank Highway Research Center, 2006.

Graybeal, Ben, *Tech Note: Design and Construction of Field-Cast UHPC Connections*. Virginia: Turner-Fairbank Highway Research Center, 2014.

Harman, Thomas, *Every Day Counts: An Innovation Partnership with States,* www.fhwa.dot.gov, 2016.

Hsu, T.C., F.O. Slate, G.M. Sturman, and G. Winter, J. ACI, Proc., Vol. 60, no. 2: 209-223.

Keierleber, Brian, Dean Bierwagen, Terry Wipf and Ahmad Abu- Hawash,

"FHWA, Iowa optimize pi girder", *Aspire Winter, 2010*.

Kosmatka, Steven and Michelle Wilson, *Design of Control of Concrete Mixtures*, EBOO1, 15th Edition. Illinois: Portland Cement Association, 2011.

Leonard, Mark, *EDC Ultra-High Performance Concrete Connections for Prefabricated Bridge Elements*, FHWA-16-CAI-09, 2016.

Li, Victor C. and Mo Li, "High-Early-Strength Engineered Cementitious Composites for Fast, Durable Concrete Repair—Material Properties", *ACI Materials Journal January – February,* (2011): 3-12.

Maso, J.C. *Proceedings of the Seventh International Congress on the Chemistry of Cements*. Paris: Editions Septima, 1980.

Mehta, P. Kumar and Paulo Monteiro, *Concrete Microstructure, Properties, and Materials* 4th Edition. Ohio: McGraw-Hill Education, 2014.

Powers, T.C., J. Am. Ceram. Soc., Vol. 41, no. 1, pp.1-6, 1958.

Powers, T.C., *The Physical Structure and Engineering Properties of Concrete,* Bulletin 90, Portland Cement Association, Skokie, IL, 1958.

Report ACI 554.1R-82, *Concr. Int.,* Vol. 4, no. 5 (1982): 9-30.

Report ACI 544.3R-84, *J. ACI, Proc.,* Vol. 81, No.2, pp. 140-48, 1984.

Shah, S.P. and B.V. Rangan, *J. ACI, Proc*. 68, no. 2 (1971): 126-135.

Swamy, R.N., P.S. Mangat, and C.V.S.K. Rao, *Fiber Reinforce Concrete,* ACI SP-44, pp. 1-28, 1974.

Thomas, M.D.A and K.J. Folliard, "Concrete Aggregates and the Durability of Concrete," *Durability of Concrete and Cement Composites*, (2007): 247-281.

Valenza II, J.J. and G.W. Scherer, "Mechanism for Salt Scaling", *J. Am. Ceramics Soc*. 89, no. 4 (2006): 1161-1179.

Weldon et al., *Feasibility Analysis of Ultra High Performance Concrete for Prestressed Concrete Bridge Applications*. New Mexico: New Mexico Department of Transportation, 2012.

Young, Francis J., S. Mindess, R.J. Gray, A. Bentur, *The Science and Technology of Civil Engineering Materials*, Prentice Hall, Inc., New Jersey, (1998): 241-245.